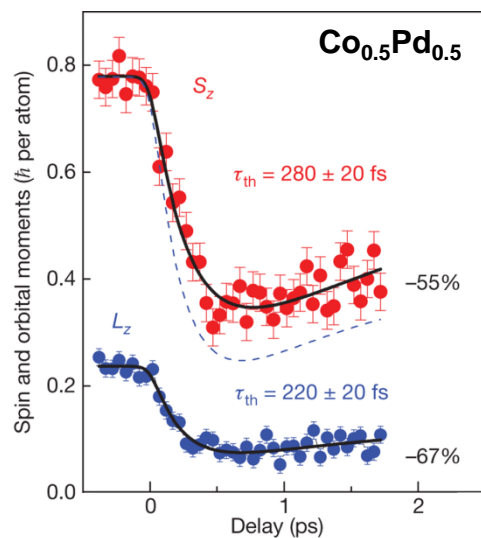
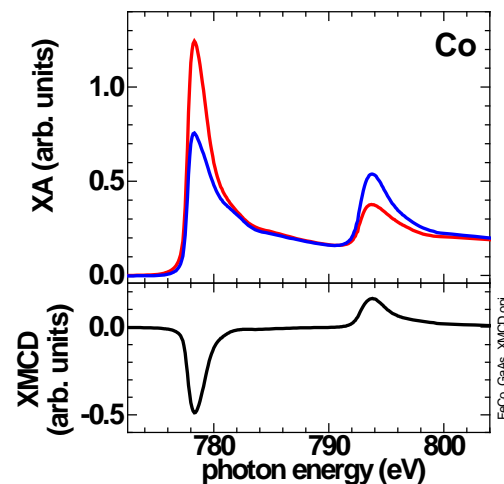
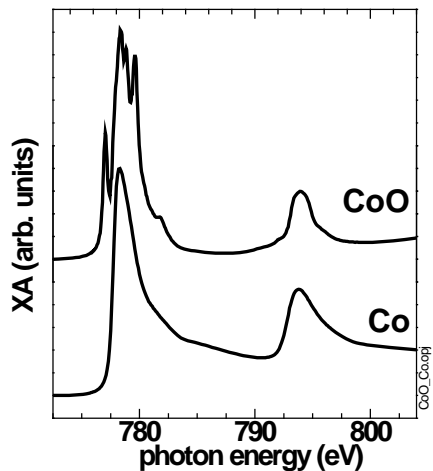
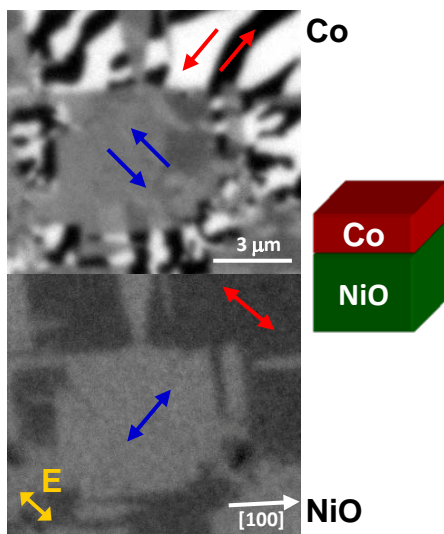
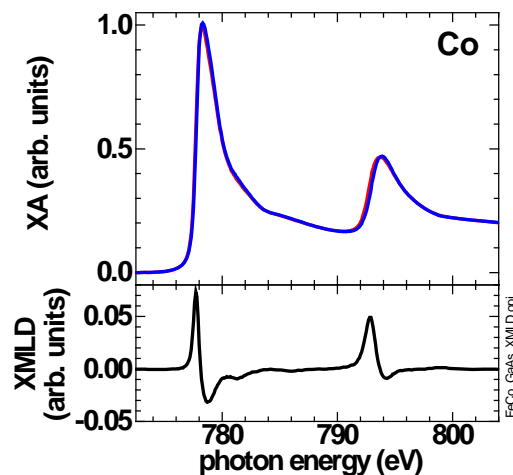
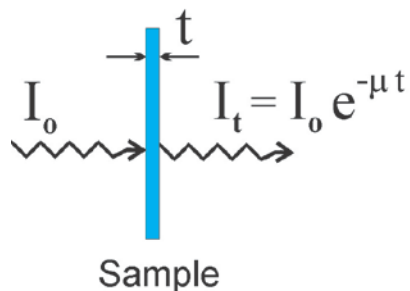


Elke Arenholz, Advanced Light Source

- + X ray absorption, XA
- + X ray magnetic circular dichroism, XMCD
- + X ray magnetic linear dichroism, XMLD
- + X ray magnetic microscopy
- + Magnetization Dynamics

C. Boeglin *et al.*, Nature **465**, 458 (2011)E. Arenholz *et al.*,
Appl. Phys. Lett. **93**, 162506 (2008)

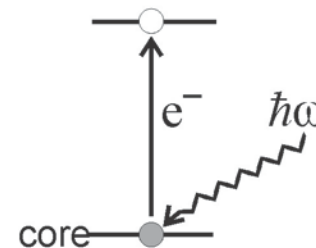


Experiment/Measurement:

Reduction in x ray flux transmitted through a sample.

X-ray absorption:

- + Electrons excited from core shells to unoccupied valence states through the absorption of a photon determined by energy and angular momentum conservation

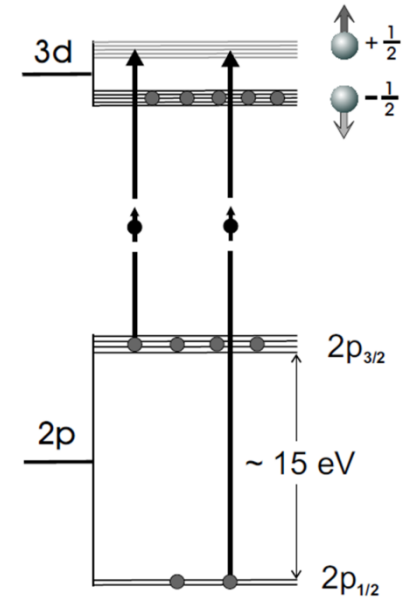


Simplest model: One electron picture

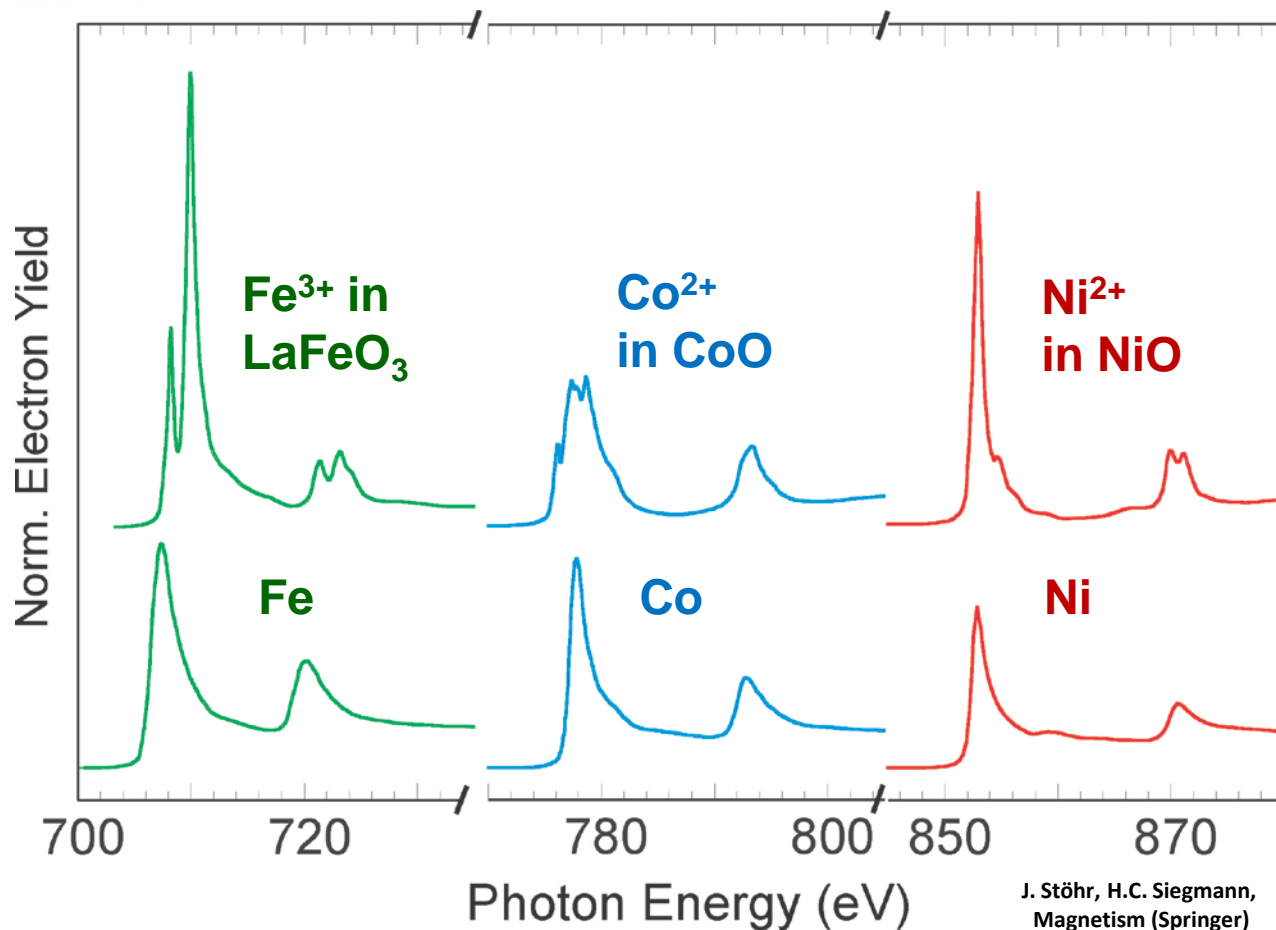
- + Photon transfers its energy and momentum to core electron
- + Core electron excited into unoccupied electronic state.
- + However: Not directly excited electrons also influenced by electron excitation, i.e. hole in core shell

Configuration model, e.g. L edge absorption :

- + Atom is excited from ground/initial state configuration, $2p^63d^n$ to excited/final state configuration, $2p^53d^{n+1}$
- + Omission of all full subshells (spherical symmetric)
- + Takes into account correlation effects in the ground state as well as in the excited state
- + Leads to multiplet effects/structure

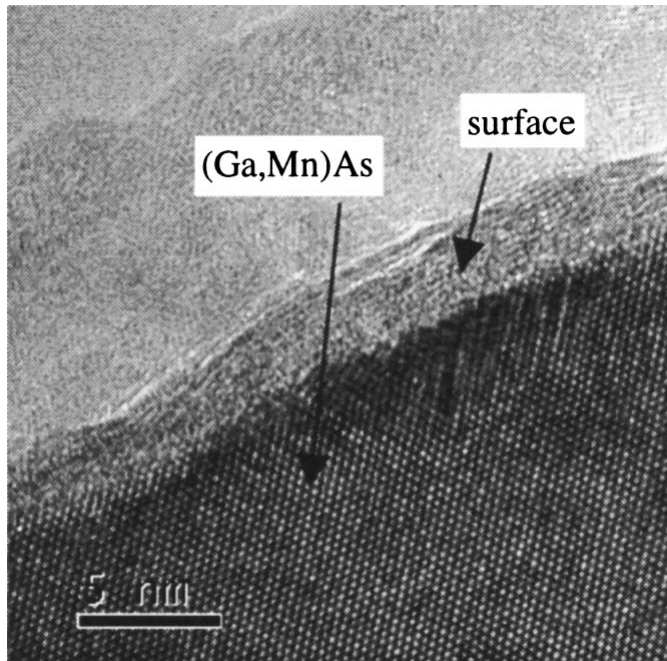


J. Stöhr, H.C. Siegmann,
Magnetism (Springer)

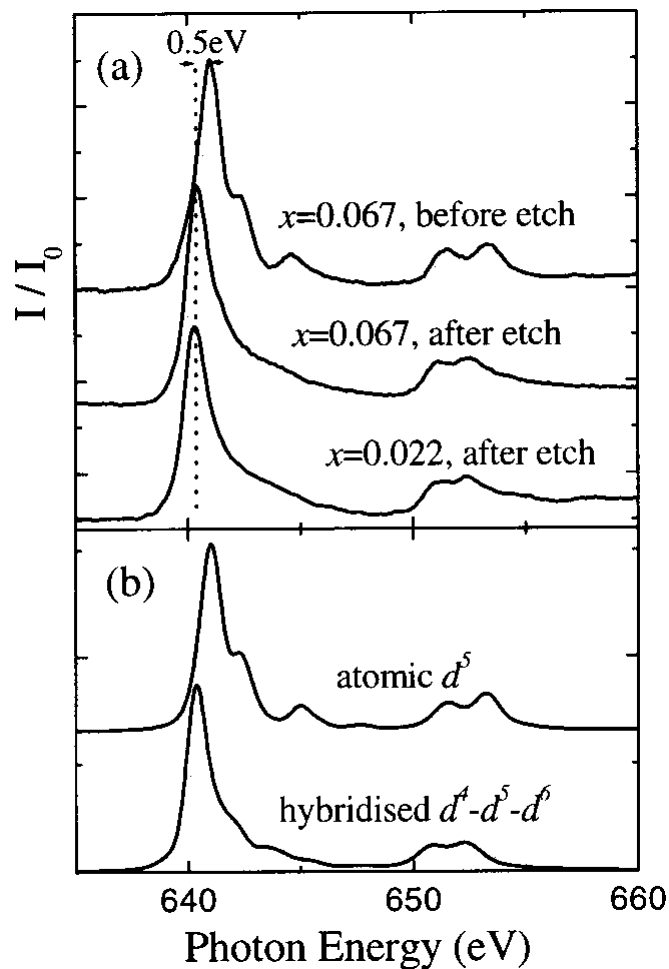


XA provides

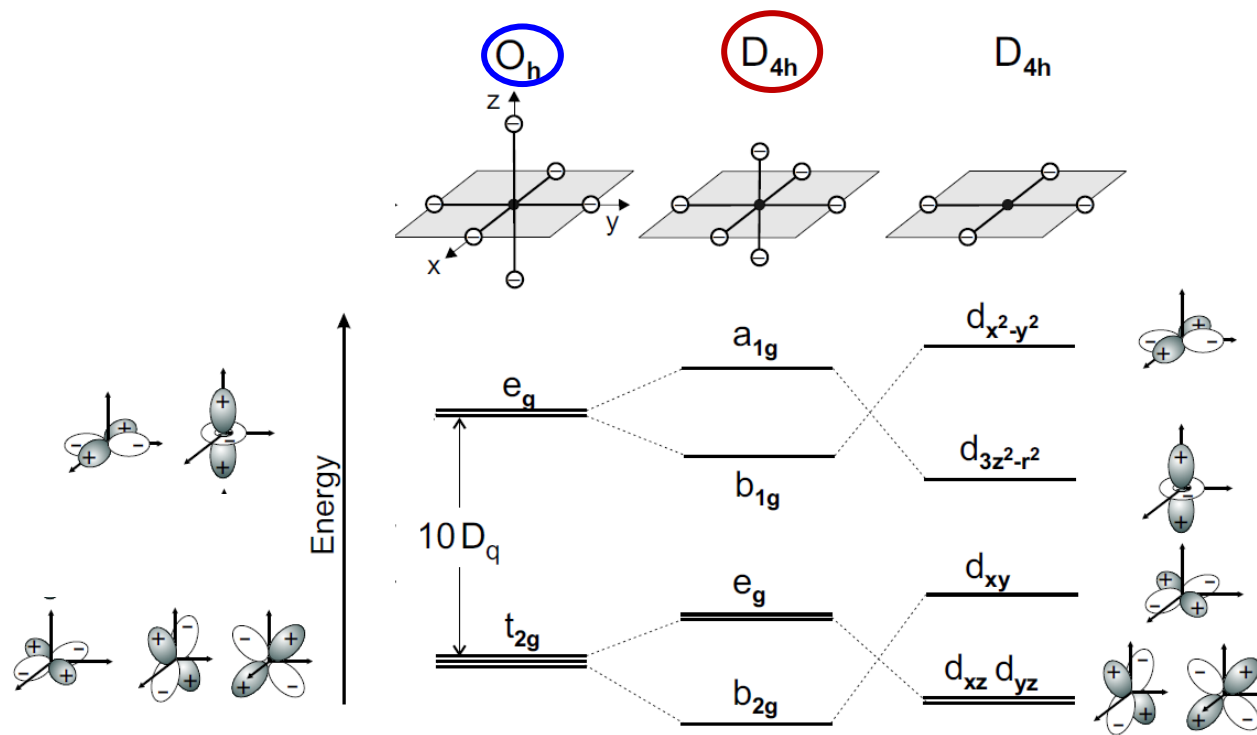
- + elemental specificity
- + sensitivity to valence shell properties, i.e. valence state and lattice site symmetry



- + As grown/before etch:
 - Multiplet structure characteristic of MnO
- + After removal of the surface layer:
 - Multiplet structure is less pronounced
 - Spectrum shifted to 0.5 eV lower photon energy.
- + Comparison with calculated spectra:
 - localized Mn ground state for the untreated sample
 - hybridized ground state after etching.



K. Edmonds *et al.*,
Appl. Phys. Lett. **84**, 4065(2004)



J. Stöhr, H.C. Siegmann,
Magnetism (Springer)

+ Electric dipole transitions: $d^0 \rightarrow 2p^5 3d^1$

+ Crystal field splitting $10Dq$ acting on 3d orbitals:

Octahedral symmetry:

e orbitals towards ligands \rightarrow higher energy

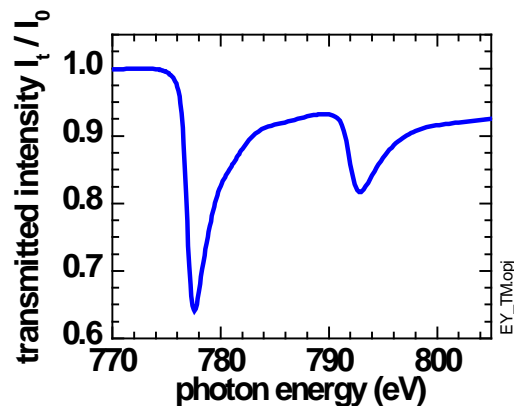
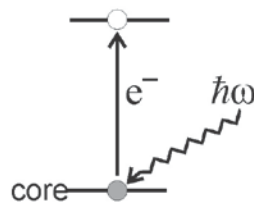
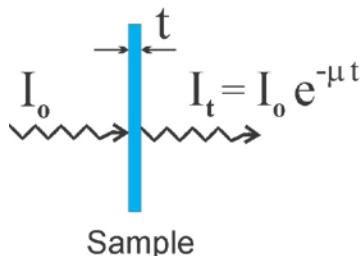
t_2 orbitals between ligands \rightarrow lower energy

Tetragonal symmetry:

e orbitals $\rightarrow b_2 = d_{xy}$, $e = d_{yz}, d_{yz}$

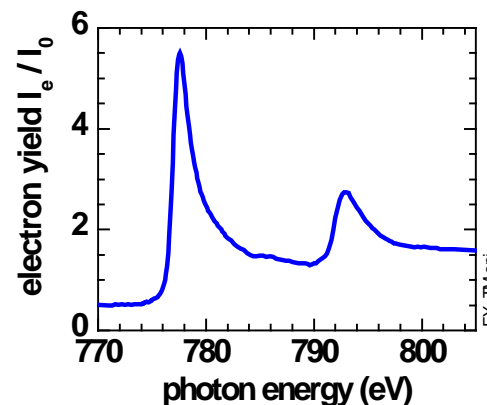
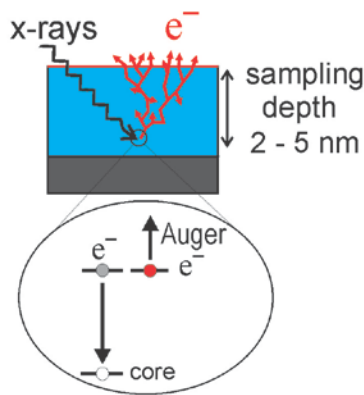
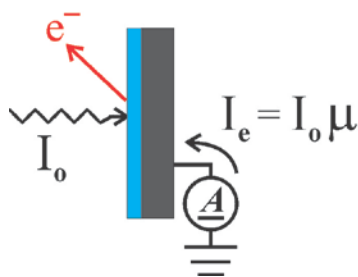
t_2 orbitals $\rightarrow b_1 = d_{x^2-y^2}$, $a_1 = d_{3z^2-r^2}$

Transmission



photons
absorbed

Electron Yield

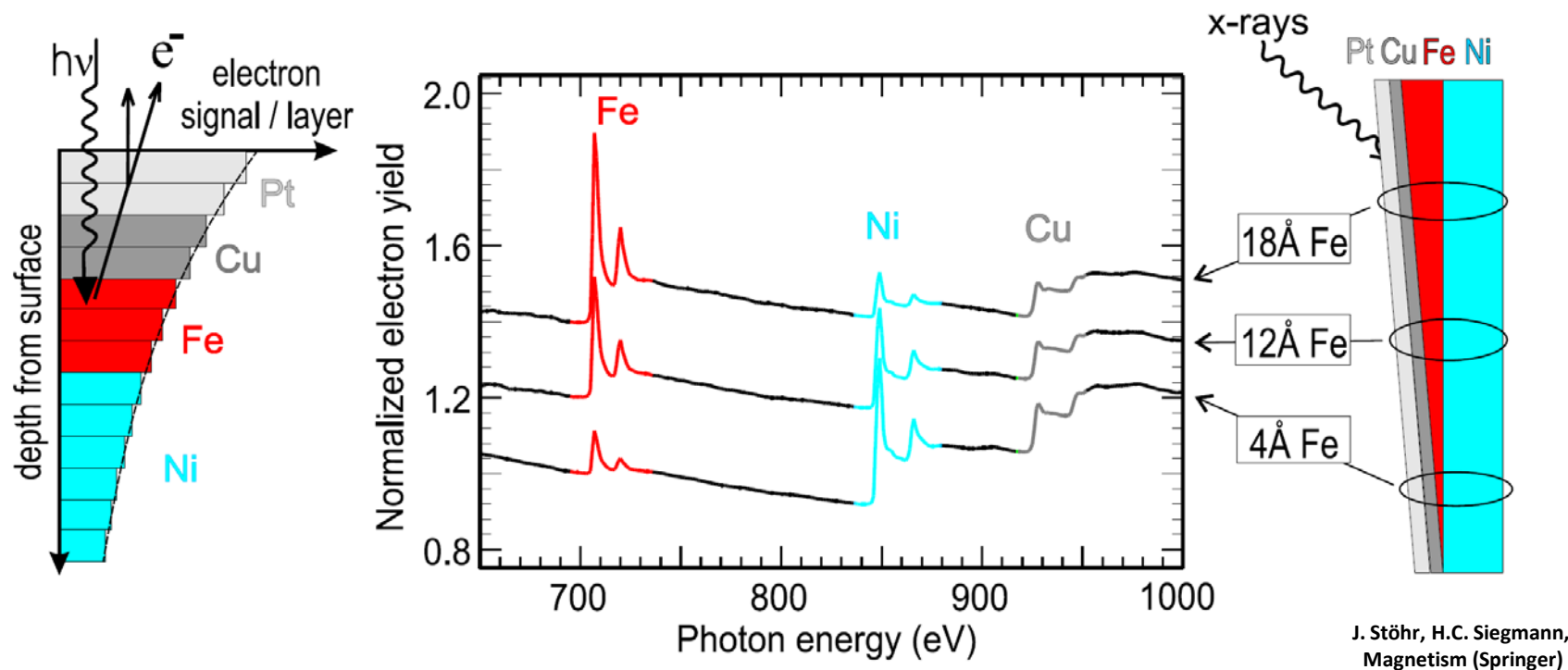


electrons
generated

J. Stöhr, H.C. Siegmann,
Magnetism (Springer)

Electron yield:

- + Absorbed photons create core holes that are filled predominantly by Auger electron emission
- + Auger electrons create low-energy secondary electron cascade through inelastic scattering
- + Emitted electrons \propto probability of Auger electron creating \propto absorption probability



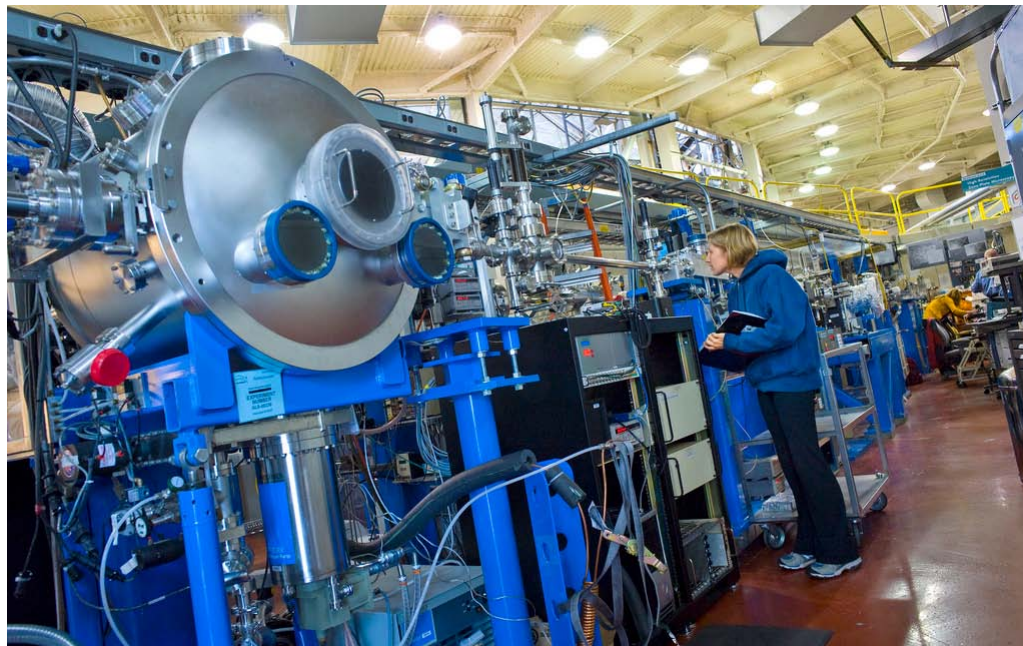
- + Electron sample depth: 2nm in Fe, Co, Ni
 - ⇒ 60% of the electron yield originates from the topmost 2nm
- + X ray absorption length: 500nm before the absorption edge
 - 20nm at the L_3 edge

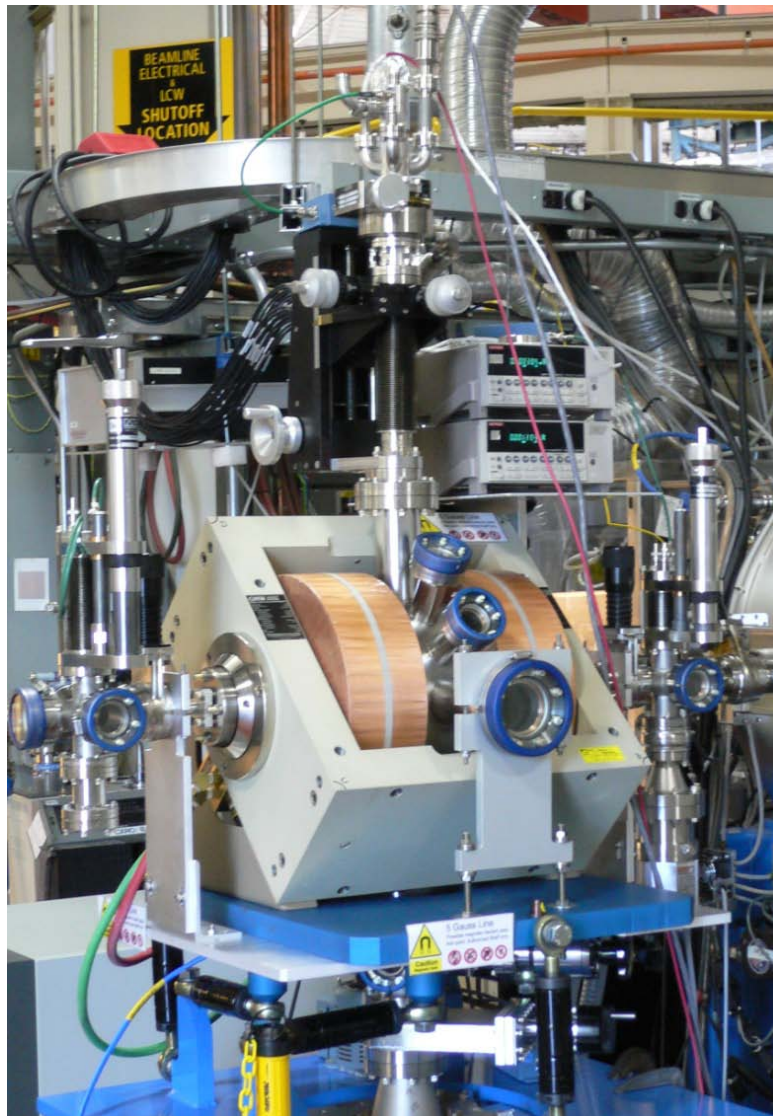
Advanced Light Source



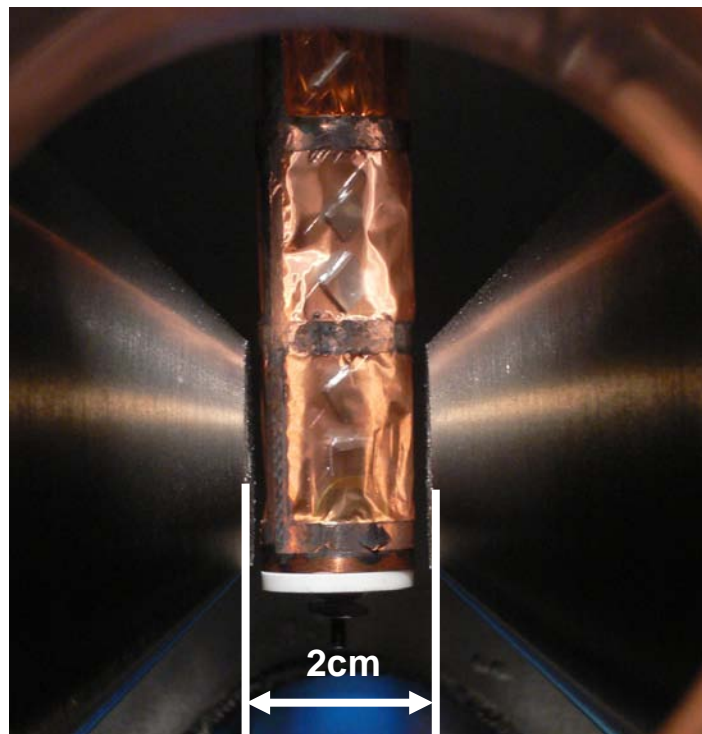
- + Tunable photon source in the soft x ray range, 200-2000eV, i.e. undulator or bend magnet, at synchrotron.
- + Beamlines/Monochromators provide photons with well defined characteristics:
 - tunable energy/wavelength
 - fixed polarization: (variable) linear, circular, elliptical, ...

BL6.3.1

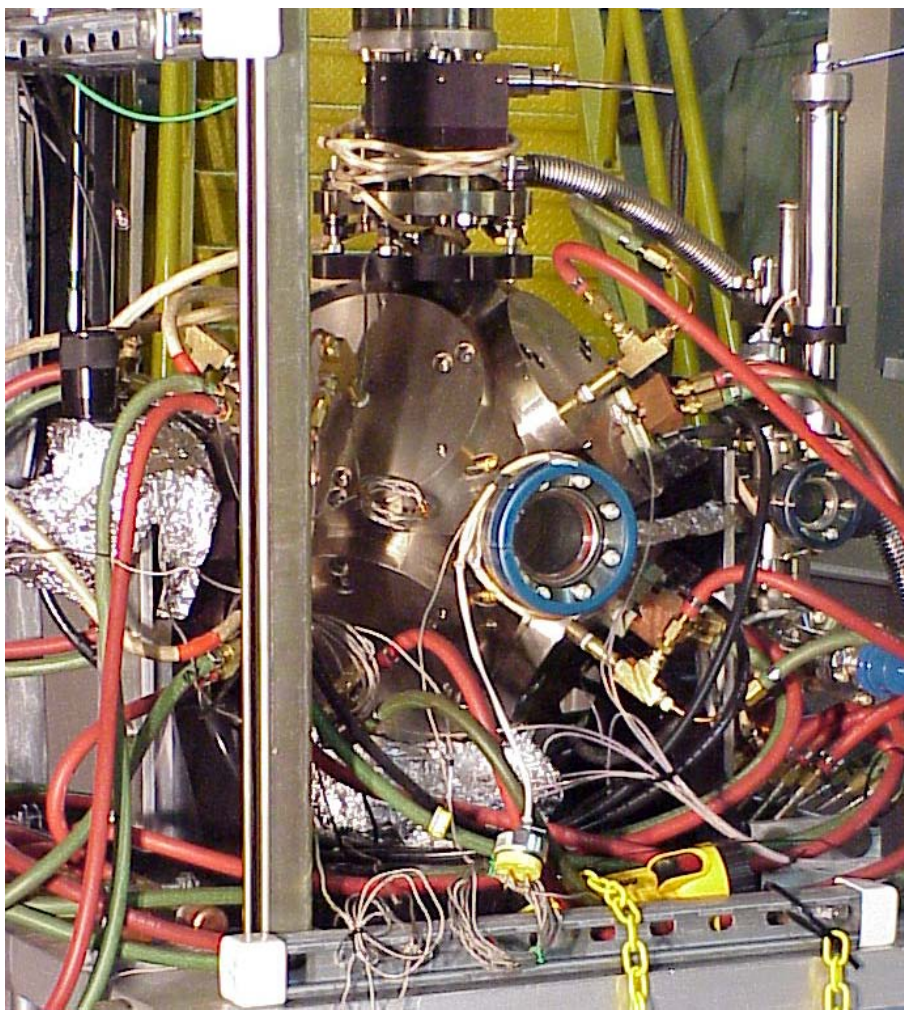




- + Endstations provide well defined sample environments for the interaction with photons:
 - precisely defined experimental geometries
 - sample temperature
 - external magnetic and electric fields
 - ...

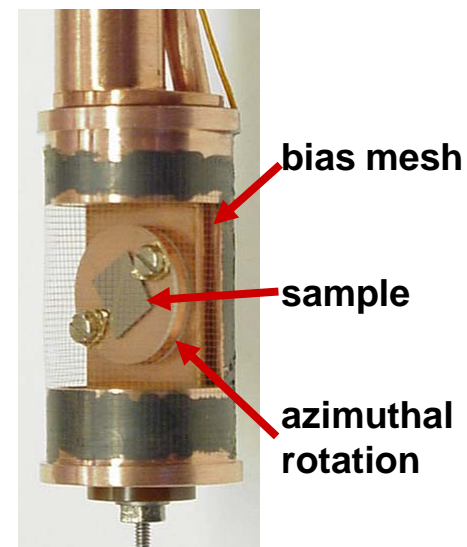
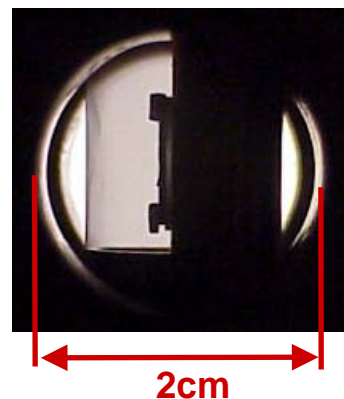
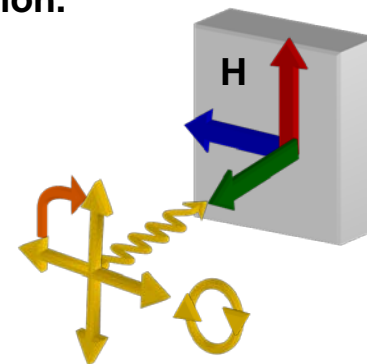
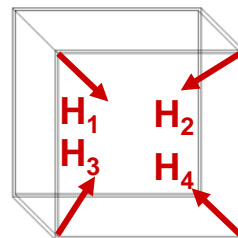


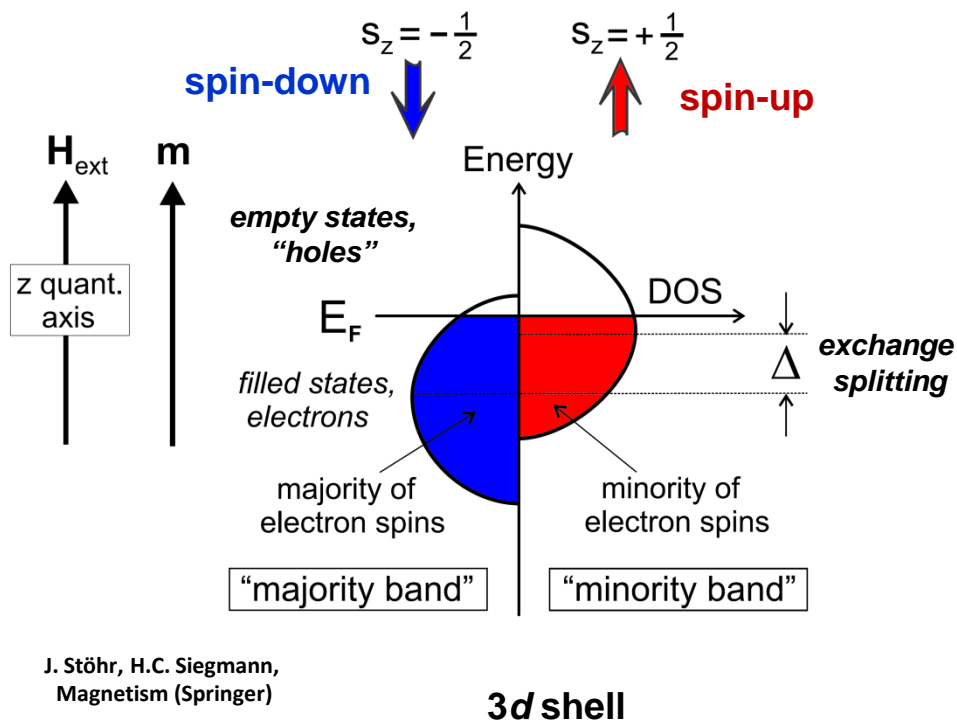
2T magnet at
ALS BL6.3.1



Vector magnet at ALS BL4.0.2

- + Magnetic fields in arbitrary directions obtained through superposition of fields generated by 4 dipole pairs in octahedral configuration.

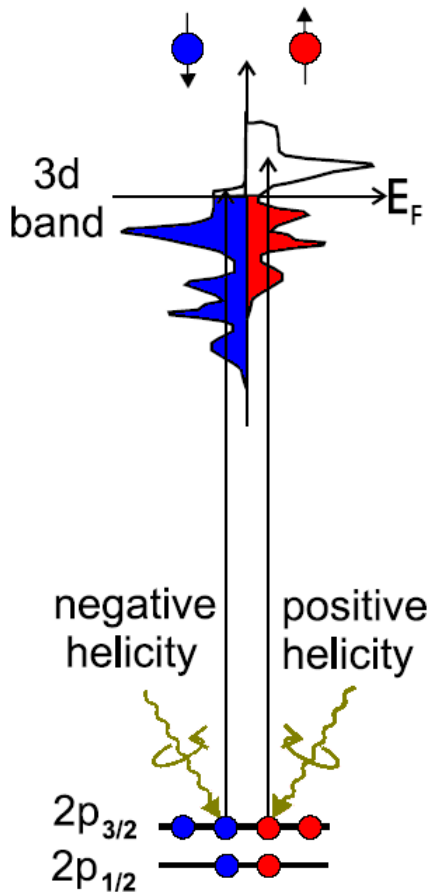




J. Stöhr, H.C. Siegmann,
Magnetism (Springer)

- + Magnetic moments in Fe, Co, Ni are well described by the Stoner model: d -bands containing up and down spins shifted relative to each other by "exchange splitting"
- + Spin- up and spin-down bands filled according to Fermi statistics.
- + Magnetic moment $|m|$ determined the difference in number of electrons in majority and minority bands

$$|m| = \mu_B (n_e^{maj} - n_e^{min})$$



J. Stöhr, H.C. Siegmann,
Magnetism (Springer)

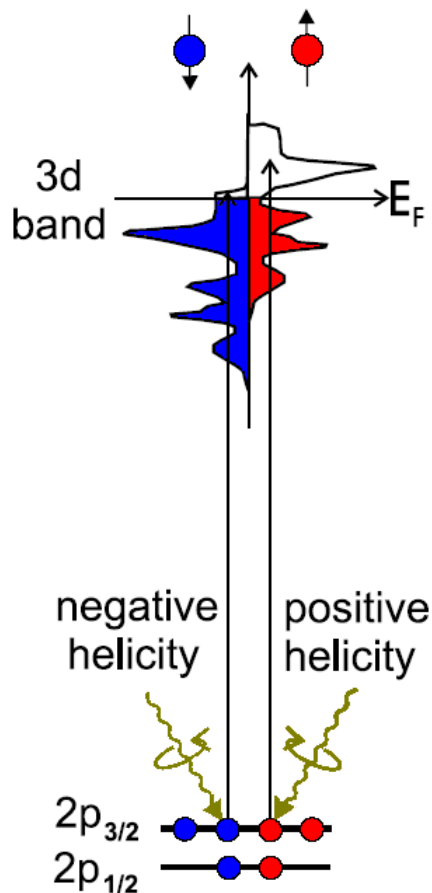
Photoelectrons excited from $2p_{3/2}$, $2p_{1/2}$ to $3d$ states

First step:

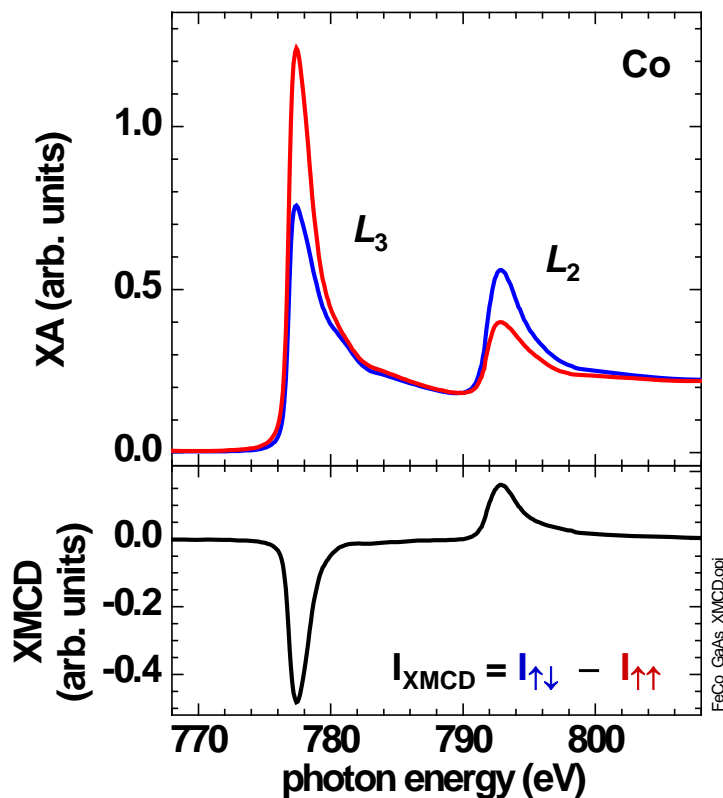
- + Excitation of electron from $2p$ states by absorption of circularly polarized x rays.
- + Note: Dipole operator does not act on the spin and
 \Rightarrow No spin flips during excitation.
- + Conservation of angular momentum
 \Rightarrow transfer of angular momentum ($\pm\hbar$) from photon to electron
- + Spin-orbit coupling: Angular momentum of photon transferred
in part to electron spin
 \Rightarrow Excited photoelectrons are spin polarized

Second step:

- + Unequal spin-up and spin-down populations
determines spin or orbital momentum of possible excitations



J. Stöhr, H.C. Siegmann,
Magnetism (Springer)

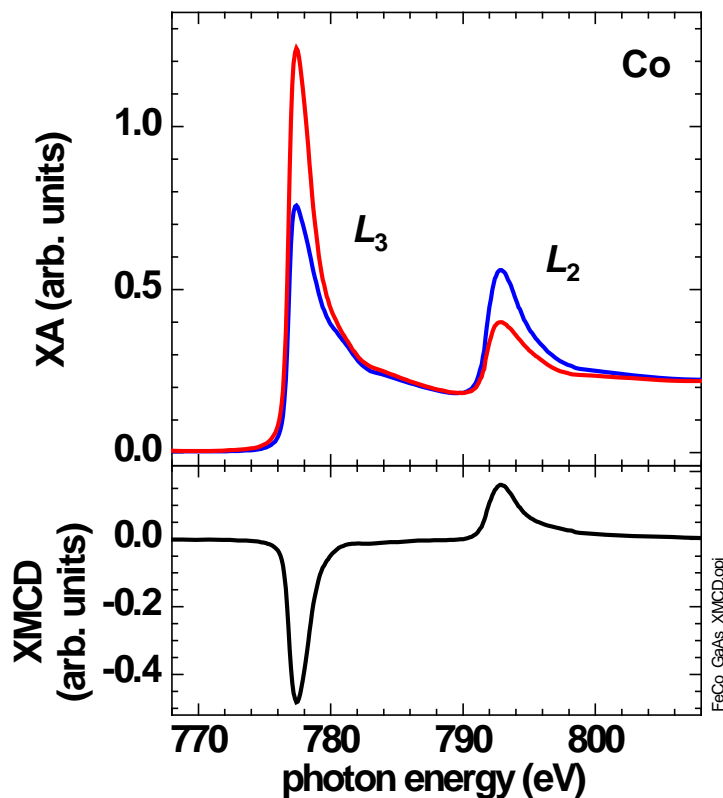
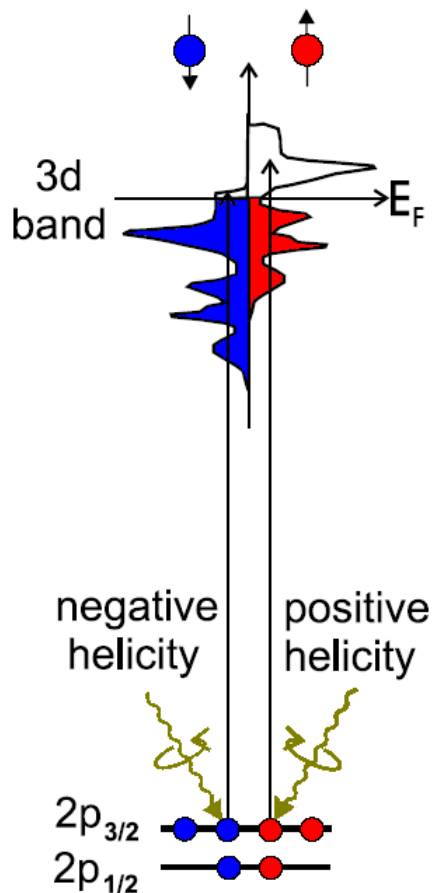


Magnitude of the dichroism effect depends on

- + degree of circular photon polarization, P_{circ}
- + angle θ between photon angular momentum, L_{ph} and magnetic moment, m
- + expectation value of 3d magnetic moment

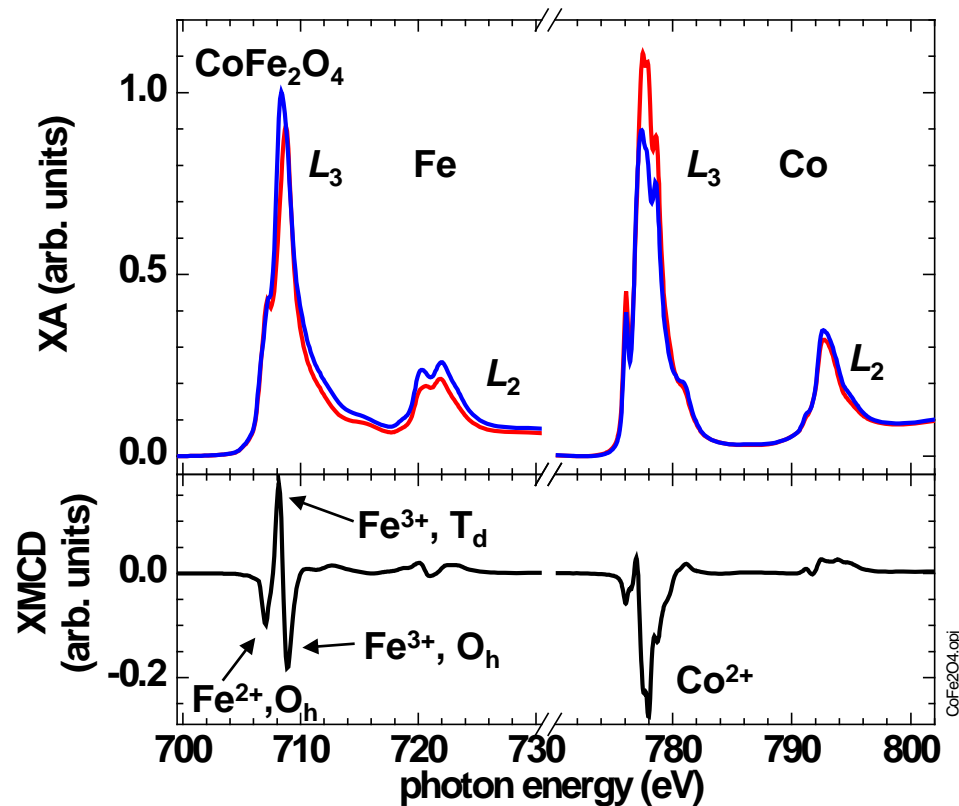
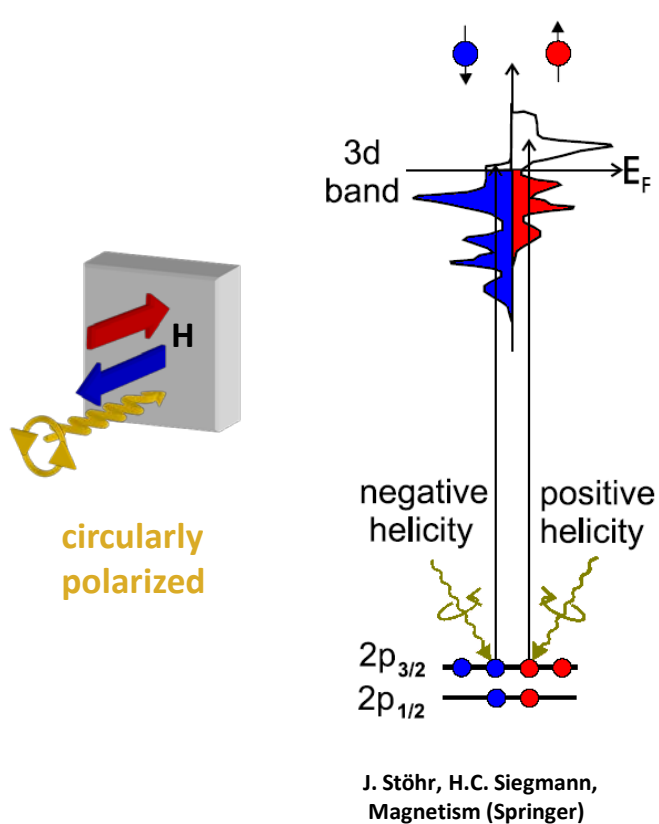
$$I_{\text{XMCD}} \propto P_{\text{circ}} \langle m \rangle \cos \theta$$

- + XMCD allows studying ferri- and ferromagnets.



- + $2p_{3/2}$ and $2p_{1/2}$ have opposite spin orbit coupling ($l+s$, $l-s$)
 \Rightarrow Spin polarization and XMCD have opposite sign at two edges
- + Spin polarization opposite for x rays with opposite helicity, i.e. photon spin, $\pm\hbar$
 \Rightarrow XMCD reverses sign with polarization
- + Reversing the x ray polarization is equivalent to reversing magnetization/ spin direction

J. Stöhr, H.C. Siegmann,
Magnetism (Springer)

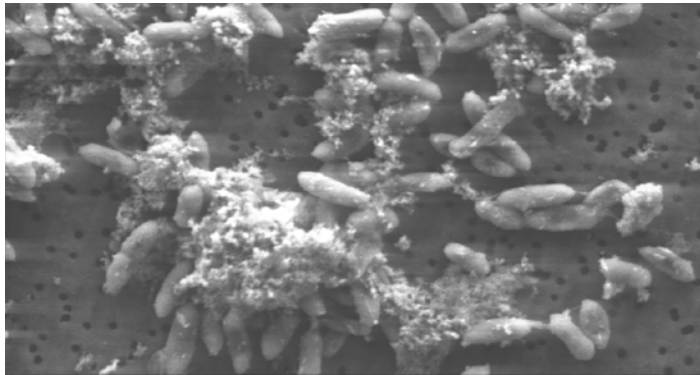


+ XMCD provides magnetic information resolving elements Fe, Co, ...

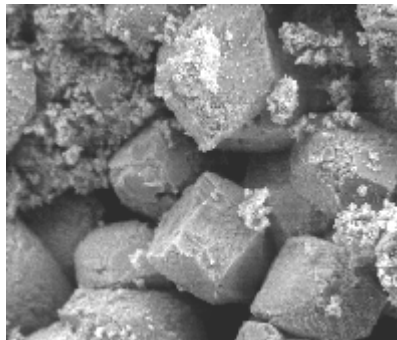
valence states: Fe²⁺, Fe³⁺, ...

lattice sites: octahedral, O_h, tetrahedral, T_d, ...

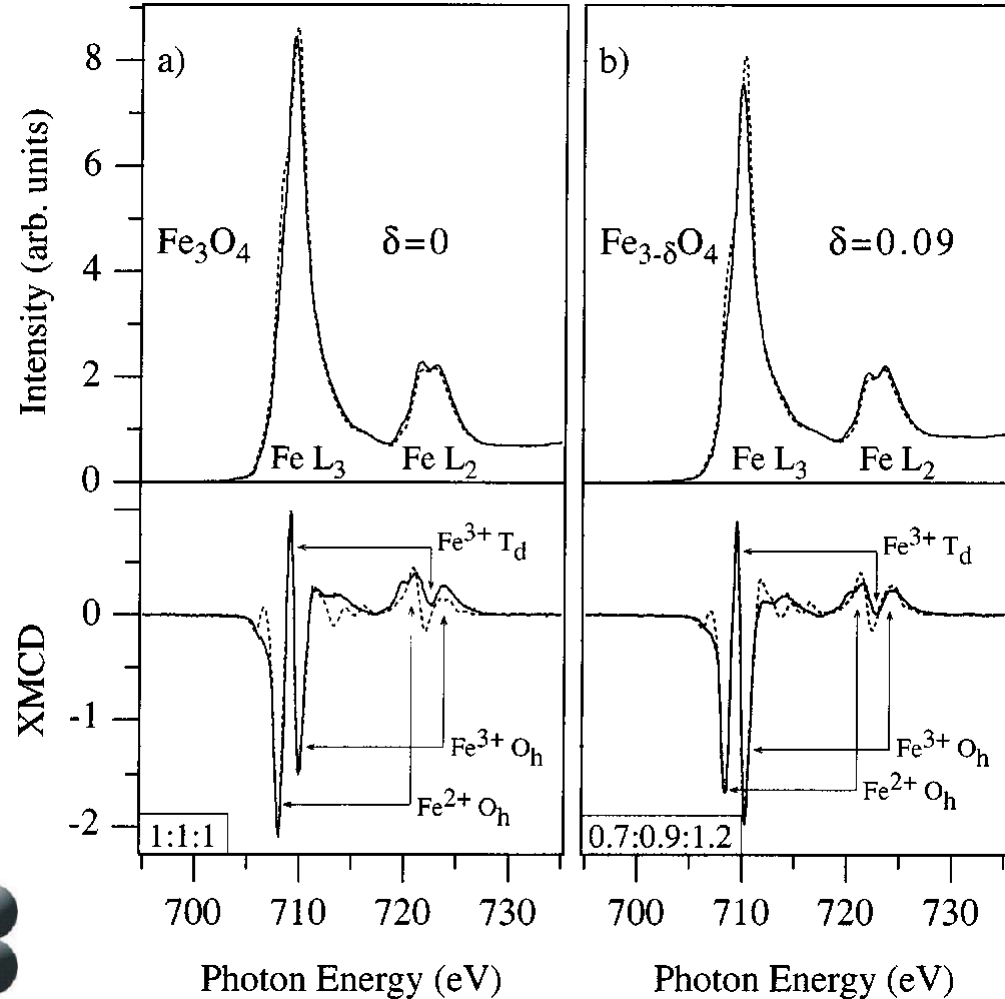
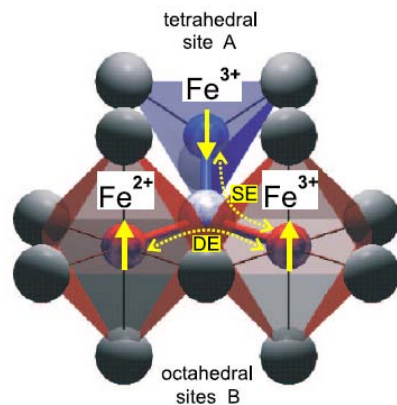
- + *Geobacter sulfurreducens* bacteria form magnetite via extracellular reduction of amorphous Fe(III)-bearing minerals



V. Cocker *et al.*,
Eur. J. Mineral. **19**, 707–716 (2007)



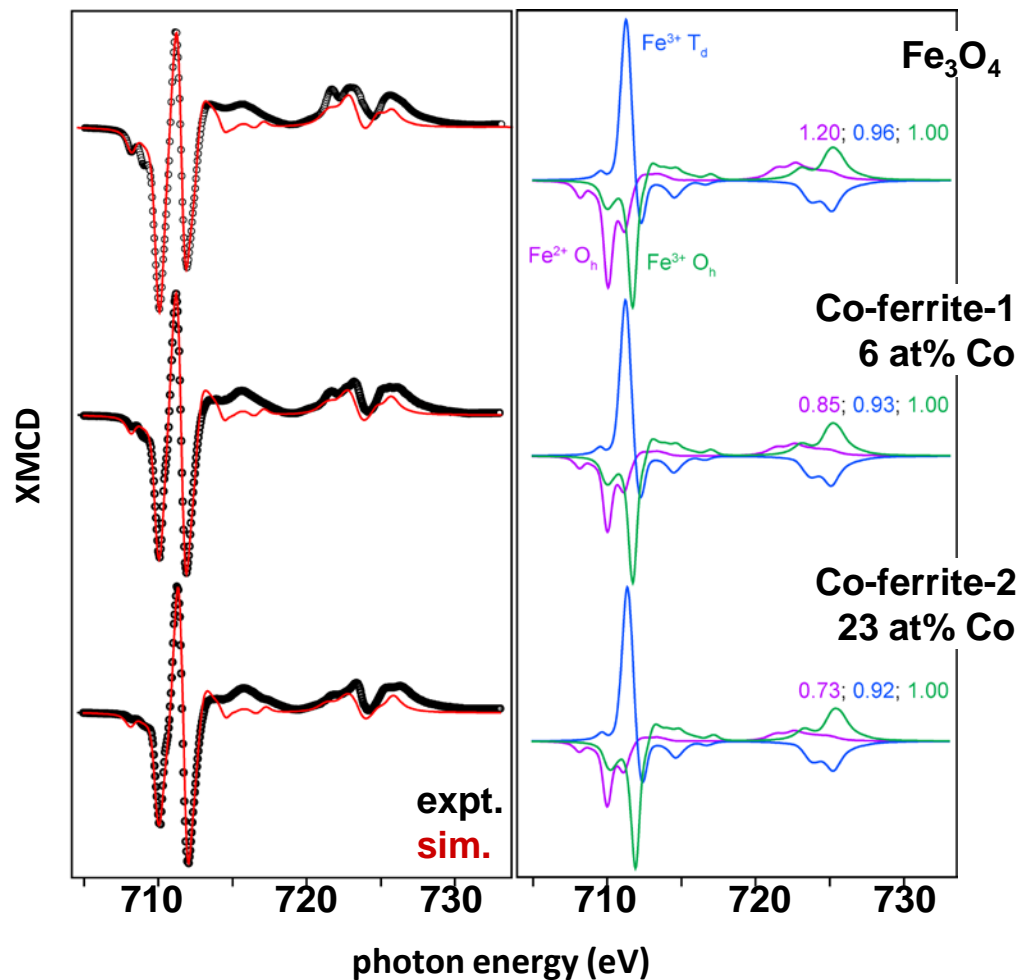
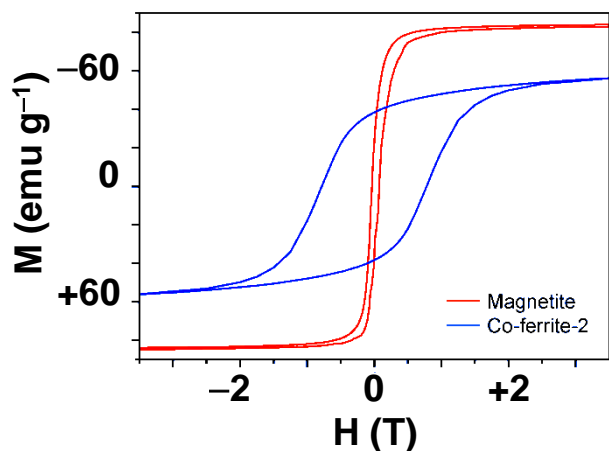
The Department of Geology and Geophysics,
University of Wisconsin-Madison



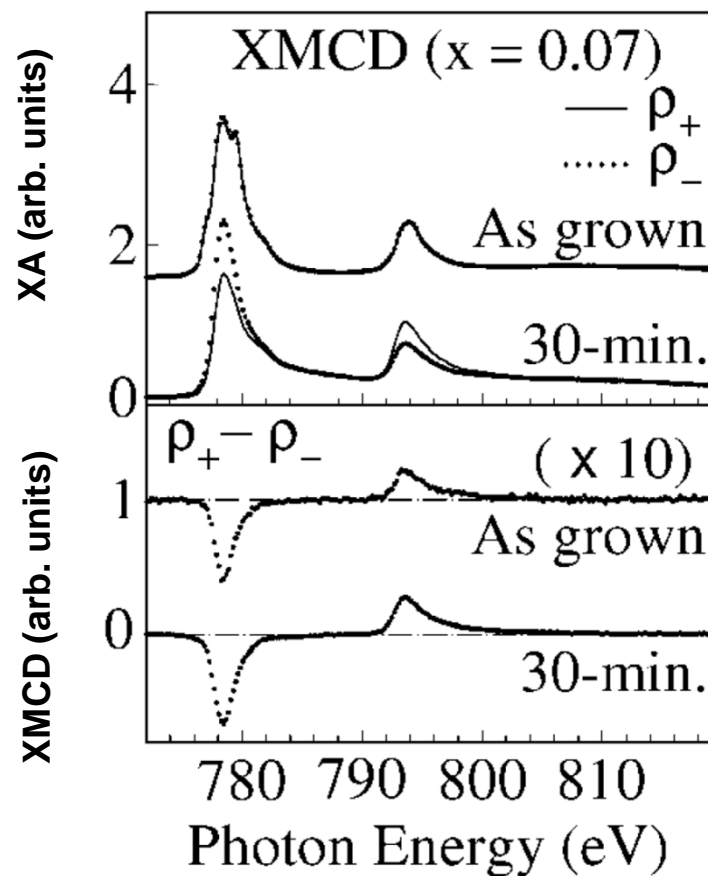
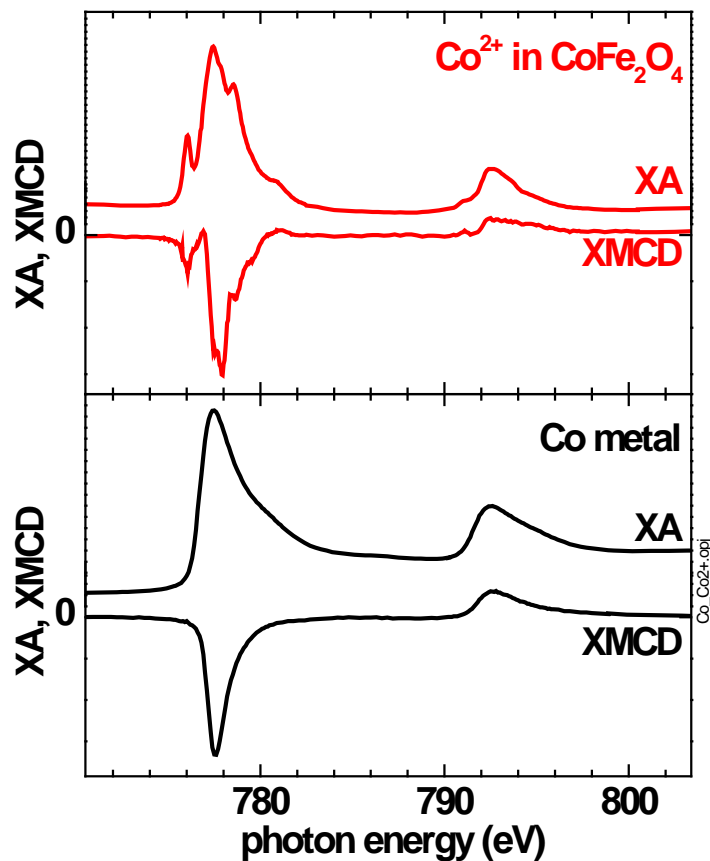
P. Morrall *et al.*,
Phys. Rev. B **67**, 214408 (2003)

Magnetite and Co ferrites produced from Co(II) containing Fe(III)-oxyhydroxides using metal-reducing bacterium (*Geobacter sulfurreducens*)

- + Up to 23at% Co²⁺ incorporated (compared to 1at% using magnetotactic bacteria)
- + Co²⁺ in Fe²⁺ O_h sites
- + 10fold increase in magnetic anisotropy

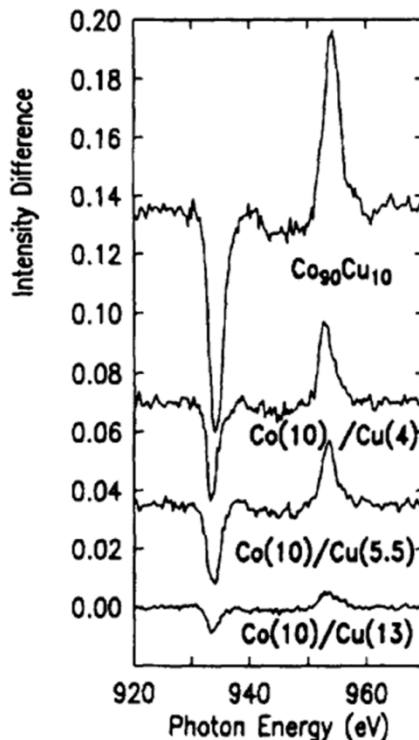
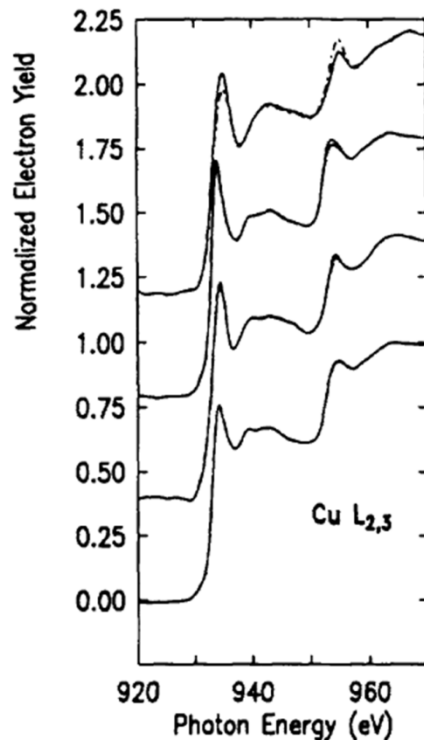
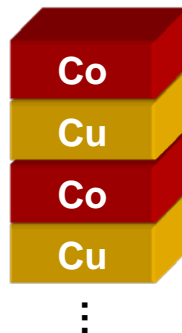
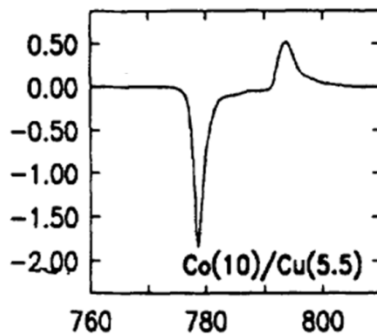
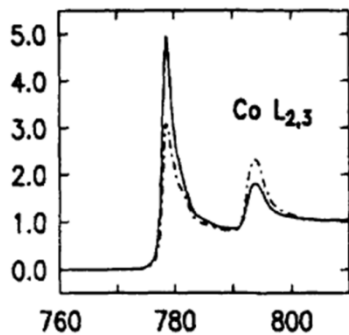


V. Cocker *et al.*,
Eur. J. Mineral. **19**, 707–716 (2007)



- + Comparing XMCD spectra with model compounds and/or theoretical multiplet calculations allows
- ⇒ Identifying the contributions to the magnetic phase of a system.

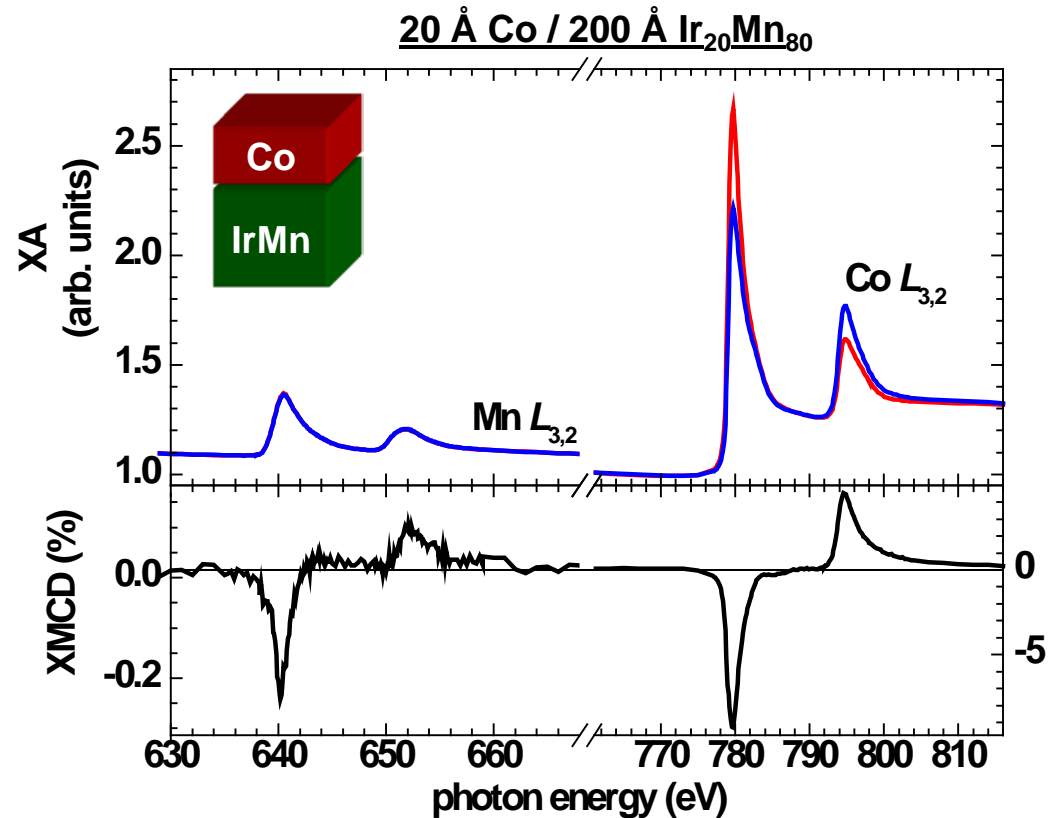
J.-Y. Kim *et al.*,
Phys. Rev. Lett. **90**, 017401 (2003)

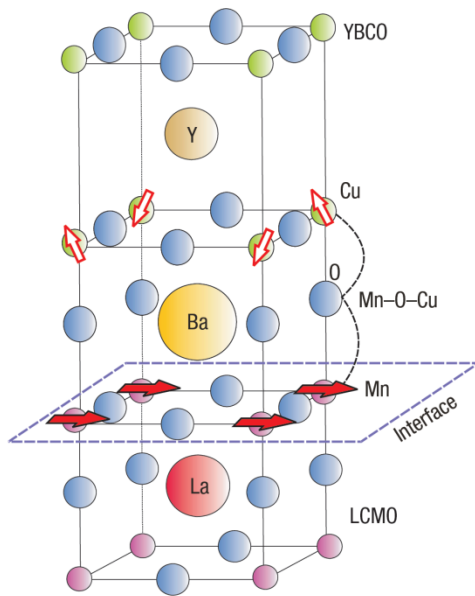
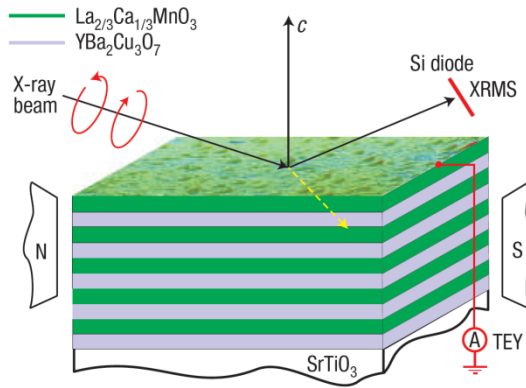


+ The element-specificity makes XMCD measurements an ideal tool to determine induced moments at interfaces between magnetic and non-magnetic elements.

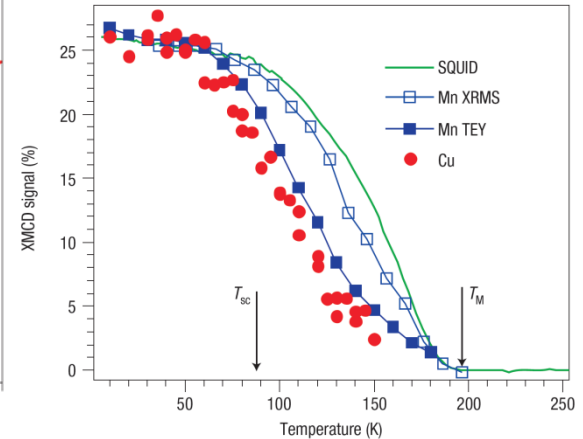
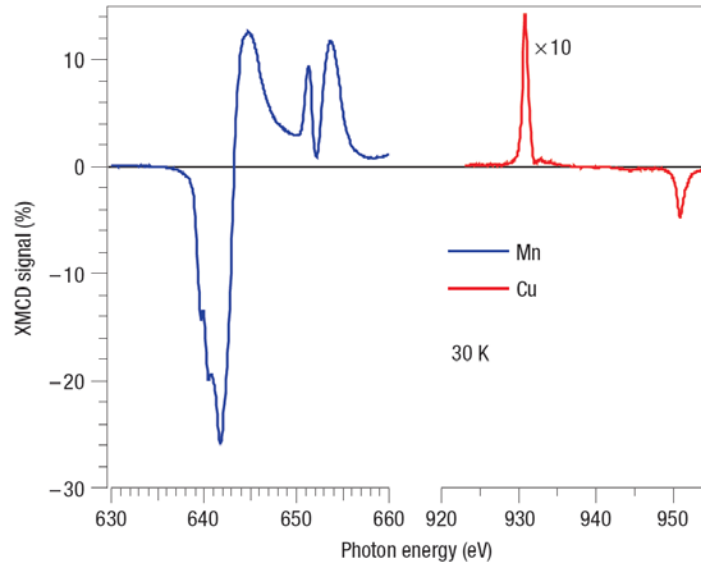
M. G. Samant *et al.*,
Phys. Rev. Lett. 72, 1112 (1994)

- + The weak Mn XMCD signal indicates uncompensated Mn at the Co/IrMn interface.
- + The same sign of XMCD signal for Co and Mn and indicates parallel coupling.
- + The nominal thickness of uncompensated interface moments is (0.5 ± 0.1) ML for Co/Ir₂₀Mn₈₀.

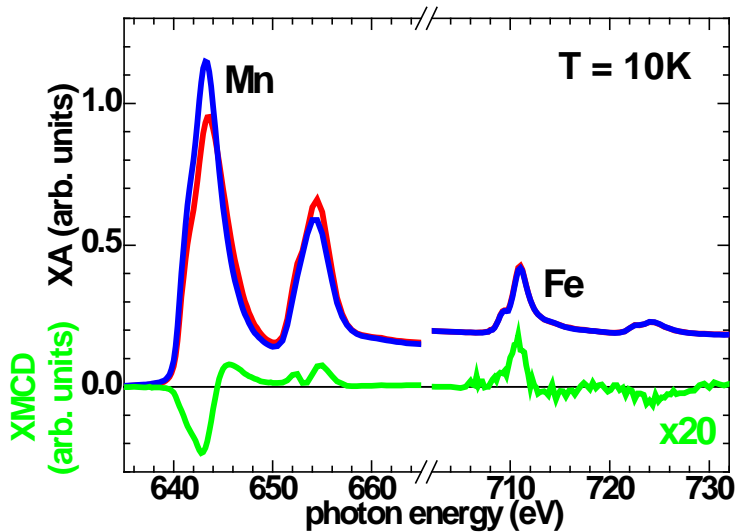




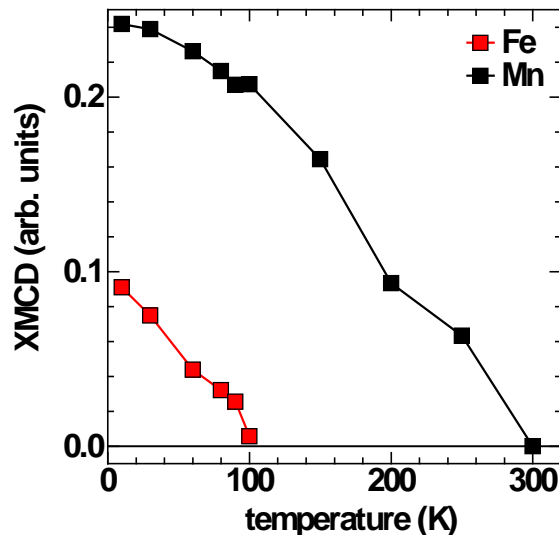
J. Chakhalian *et al.*,
Nature Phys. **2**, 244 (2006)



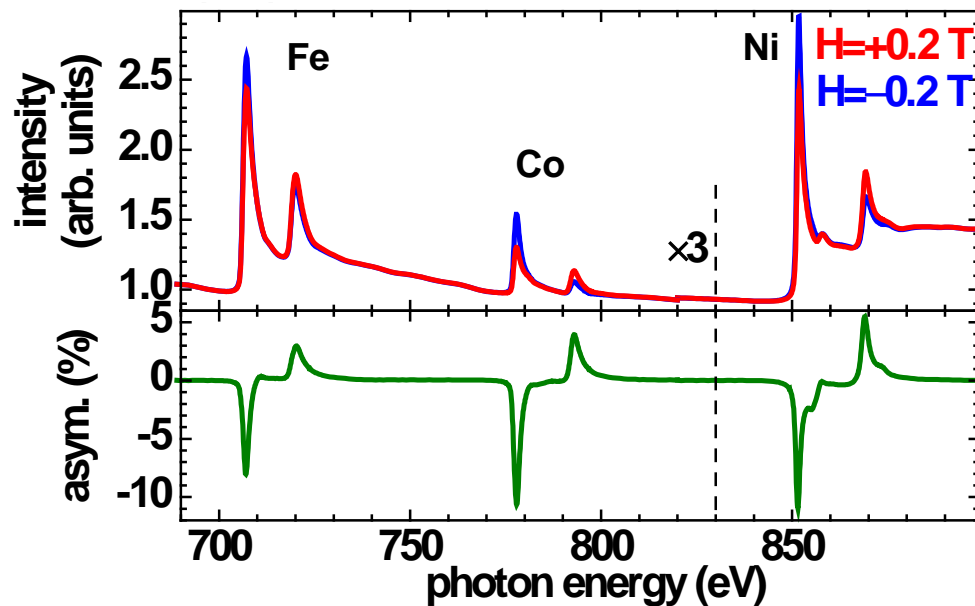
- + LCMO : significant Mn $L_{3,2}$ XMCD at $T = 30\text{K}$
ferromagnetic transition $\sim 180\text{ K}$
- + YBCO: Weak Cu $L_{3,2}$ XMCD
 \Leftrightarrow net ferromagnetic polarization on Cu
i.e. presence of uncompensated induced magnetic moment in the YBCO layer close to LCMO interface.
- + opposite sign of Cu and Mn XMCD
 \Leftrightarrow antiparallel orientation of Cu and Mn moments



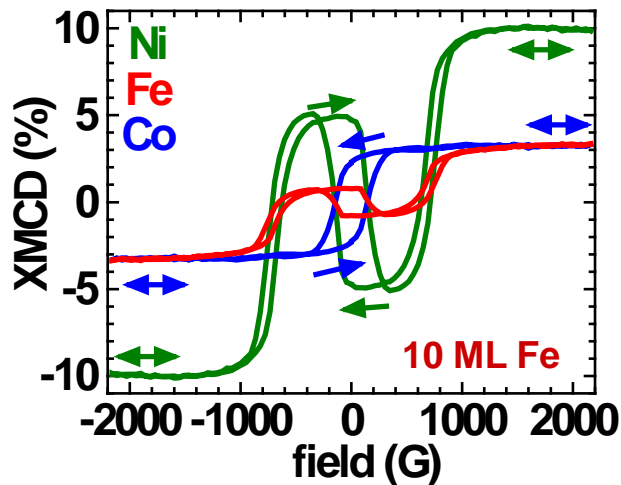
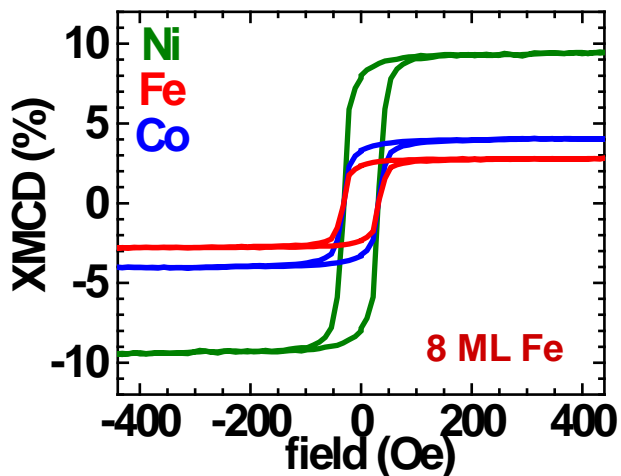
- + La_{0.7}Sr_{0.3}MnO₃ : significant Mn L_{3,2} XMCD at T = 10K
ferromagnetic transition ~300 K
- + BiFeO₃: Weak Fe L_{3,2} XMCD
⇔ net ferromagnetic polarization on Fe
i.e. presence of uncompensated induced magnetic moment in the BiFeO₃ layer close to La_{0.7}Sr_{0.3}MnO₃ interface.
- + opposite sign of Fe and Mn XMCD
⇔ antiparallel orientation of Fe and Mn moments
- + Transition temperature of the magnetic phase in BiFeO₃ significantly lower than La_{0.7}Sr_{0.3}MnO₃

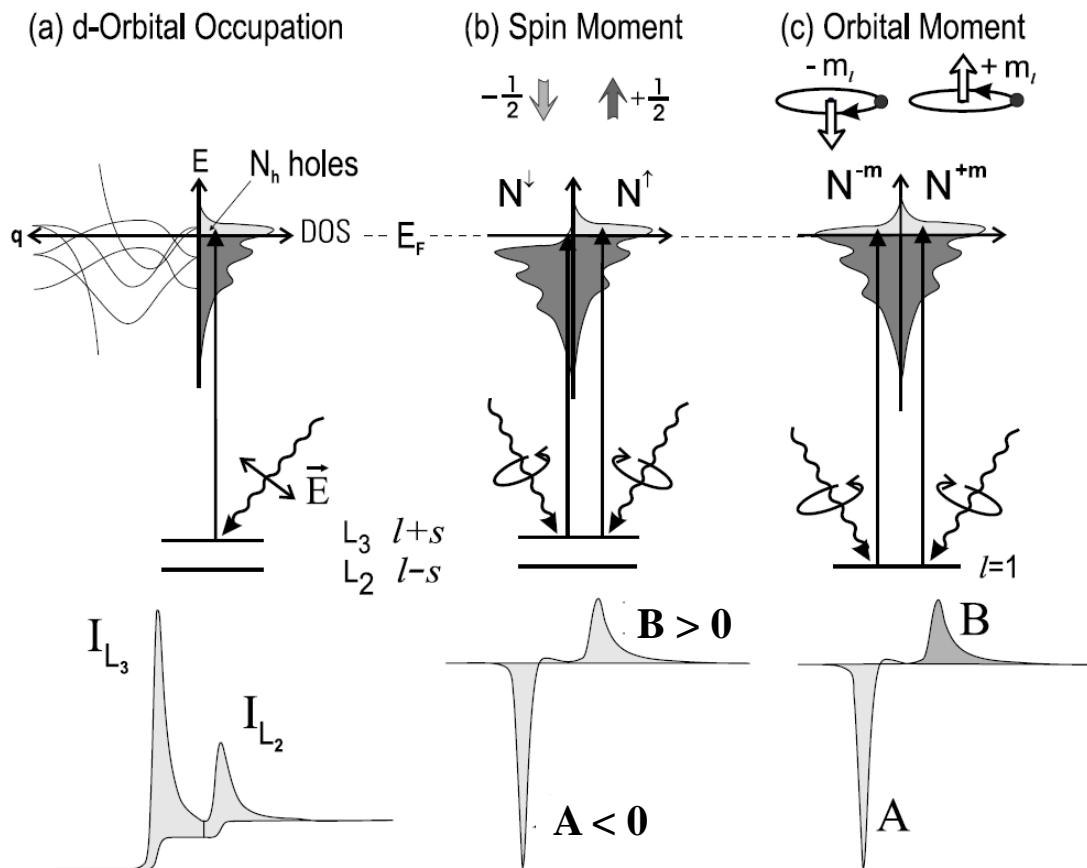


P. Yu *et al.*,
Phys. Rev. Lett. **105**, 027201 (2010)



- + Monitoring the field dependence of the XMCD signal
- ⇒ Detailed information on magnetization reversal in complex magnetic heterostructures





+ Theoretically derived sum rules correlate the XMCD spectra with the spin and orbital moment providing a unique tool for studying magnetic materials.

$$N_h = \langle I_{L_3} + I_{L_2} \rangle / C$$

$$m_S = \mu_B \langle -A + 2B \rangle / C \quad m_L = -2\mu_B \langle A + B \rangle / 3C$$

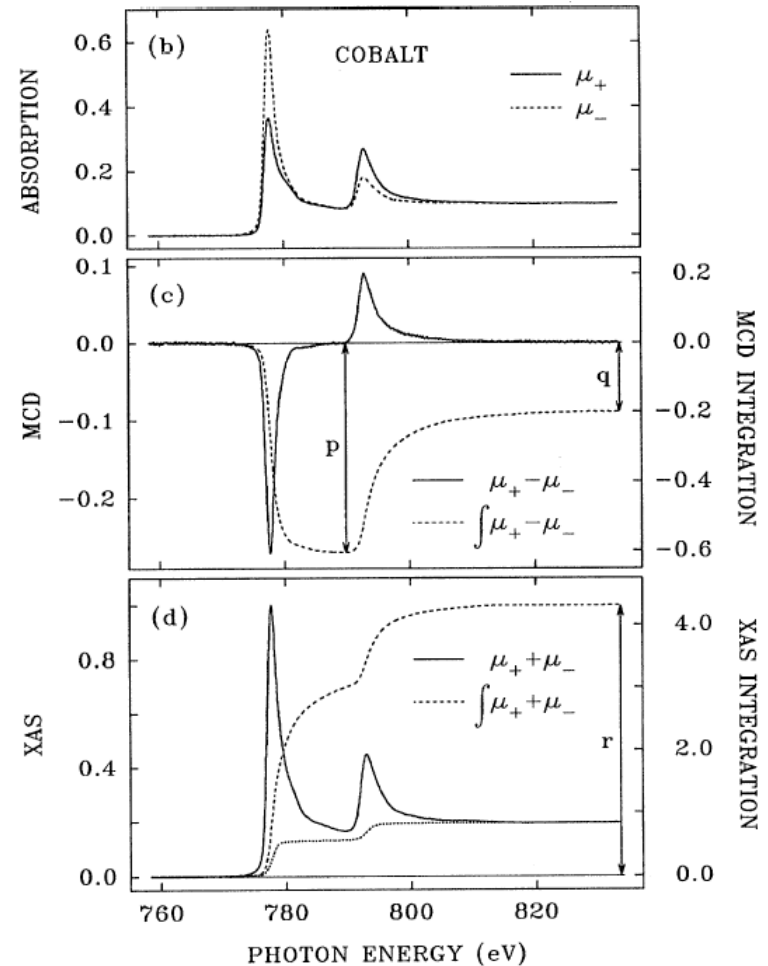
J. Stöhr, H.C. Siegmann,
Magnetism (Springer)

+ Separation of spin and orbital moments requires very high quality data.

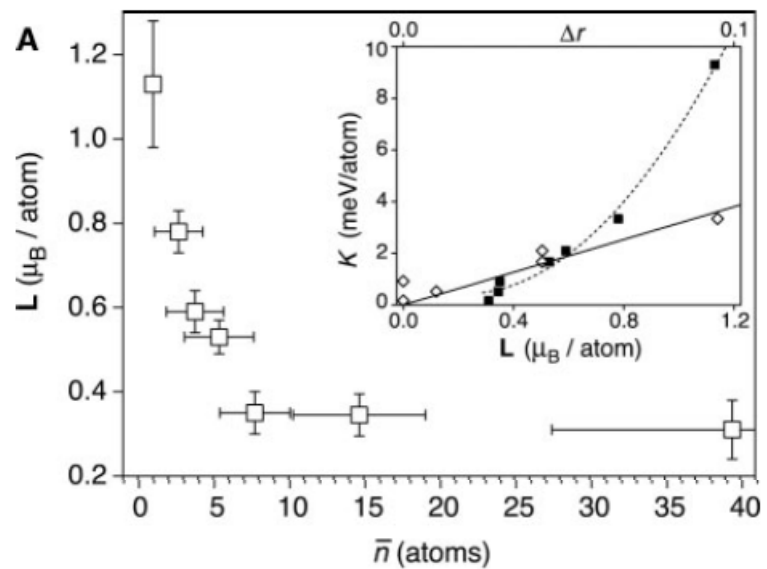
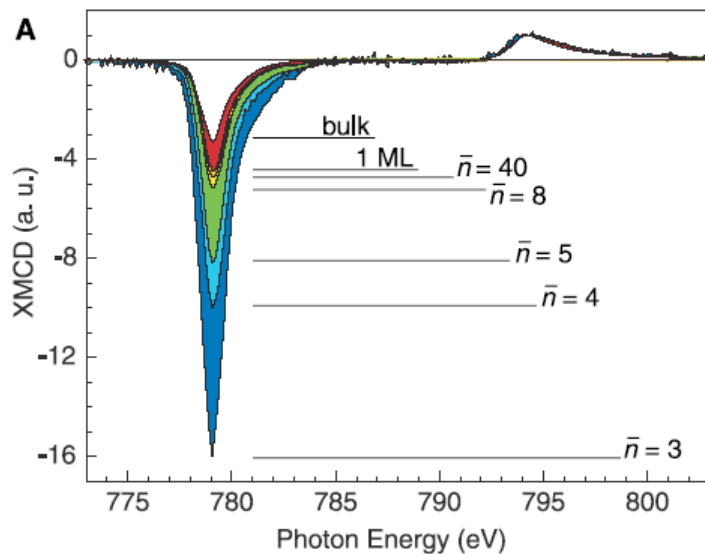
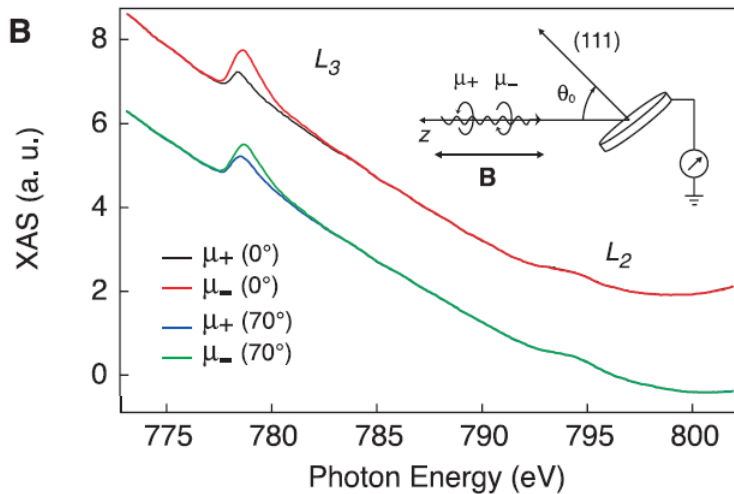
$$\frac{m_{\text{orb}}}{m_{\text{spin}}} = \frac{2q}{9p - 6q}$$

$$m_{\text{orb}} = -\frac{4q(10 - n_{3d})}{3r}$$

$$m_{\text{spin}} = -\frac{(6p - 4q)(10 - n_{3d})}{r}$$

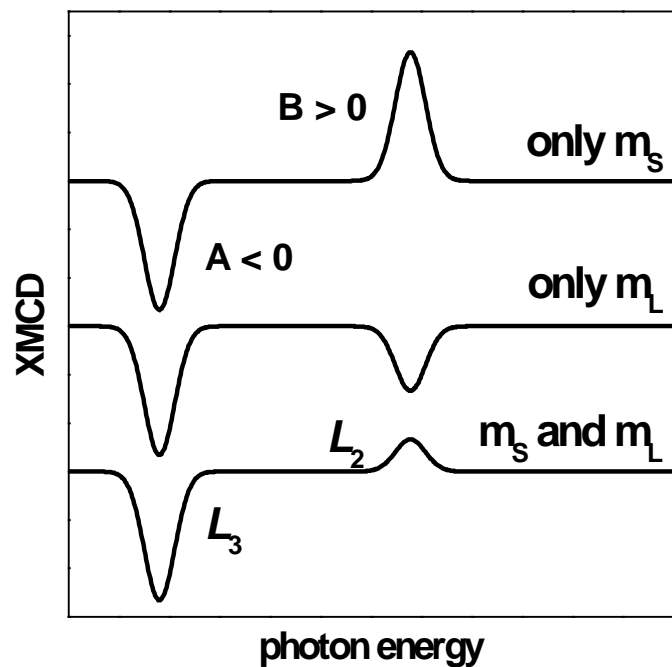


C.T. Chen *et al.*,
 Phys. Rev. Lett. **75**, 152(1995)



- + Strong variation of orbital and spin magnetic moment observable as change in L_3 and L_2 in the XMCD spectrum.
- + Co atoms and nanoparticles on Pt have enhanced orbital moments up to $1.1 \mu_B$

P. Gambardella *et al.*,
 Science **300**, 1130 (2003)

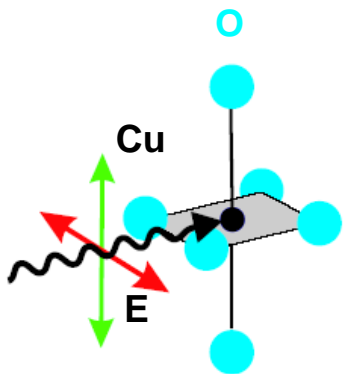


+ Spin and orbital moment only systems have distinct XMCD spectra:

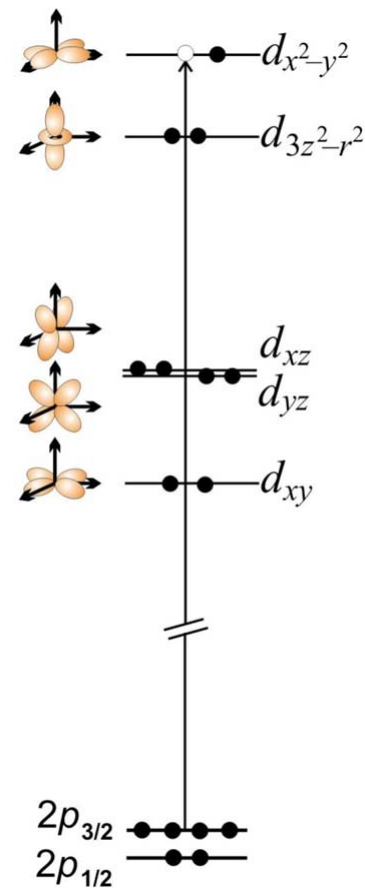
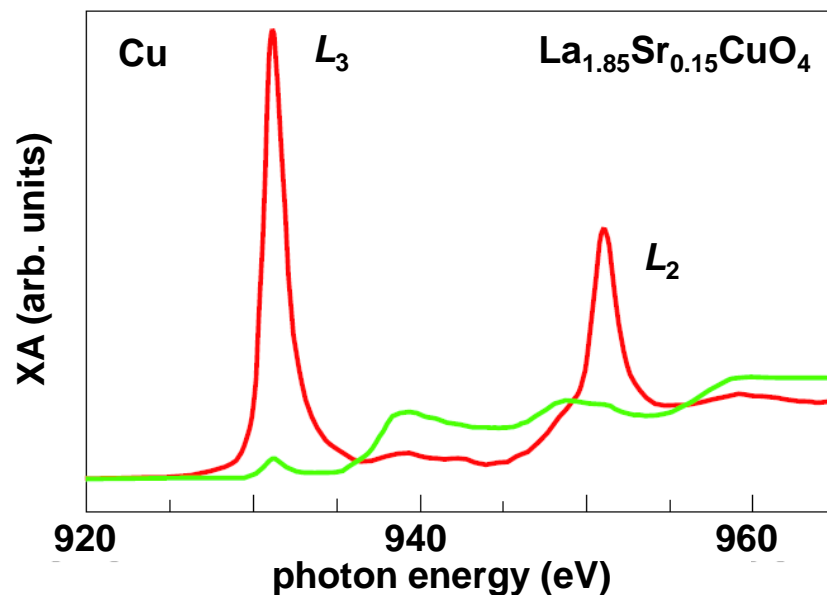
$$m_L = -2\mu_B \langle A + B \rangle / 3C = 0 \quad \text{for } A = -B$$

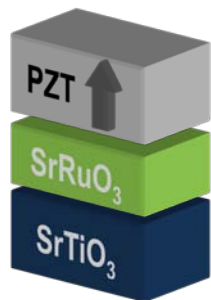
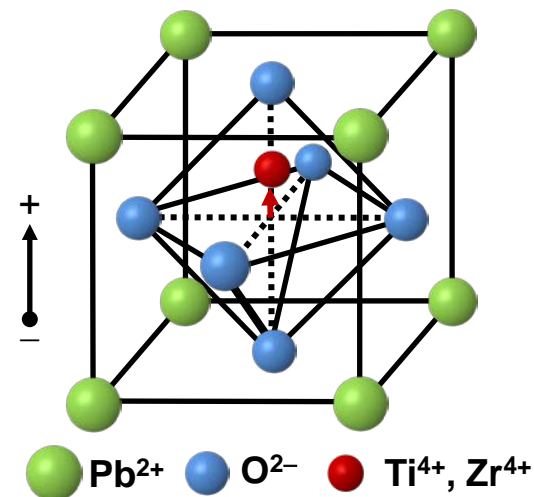
$$m_S = \mu_B \langle -A + 2B \rangle / C = 0 \quad \text{for } A = 2B$$

- + Linear dichroism: difference in x-ray absorption for different polarization direction relative to crystalline and/or spin axis.
- + Linear dichroism is due to the anisotropic charge distribution about the absorbing atom caused by bonding and/or magnetic order.
- + “Search Light Effect”:
X ray absorption of linear polarized x rays proportional to density of empty valence states in direction of electric field vector E .

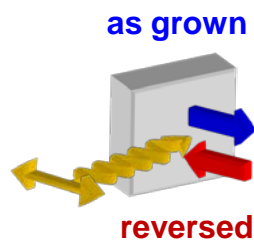
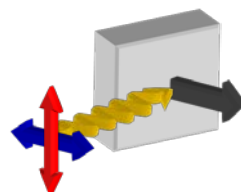


C. T. Chen *et al.*
PRL 68, 2543 (1992)



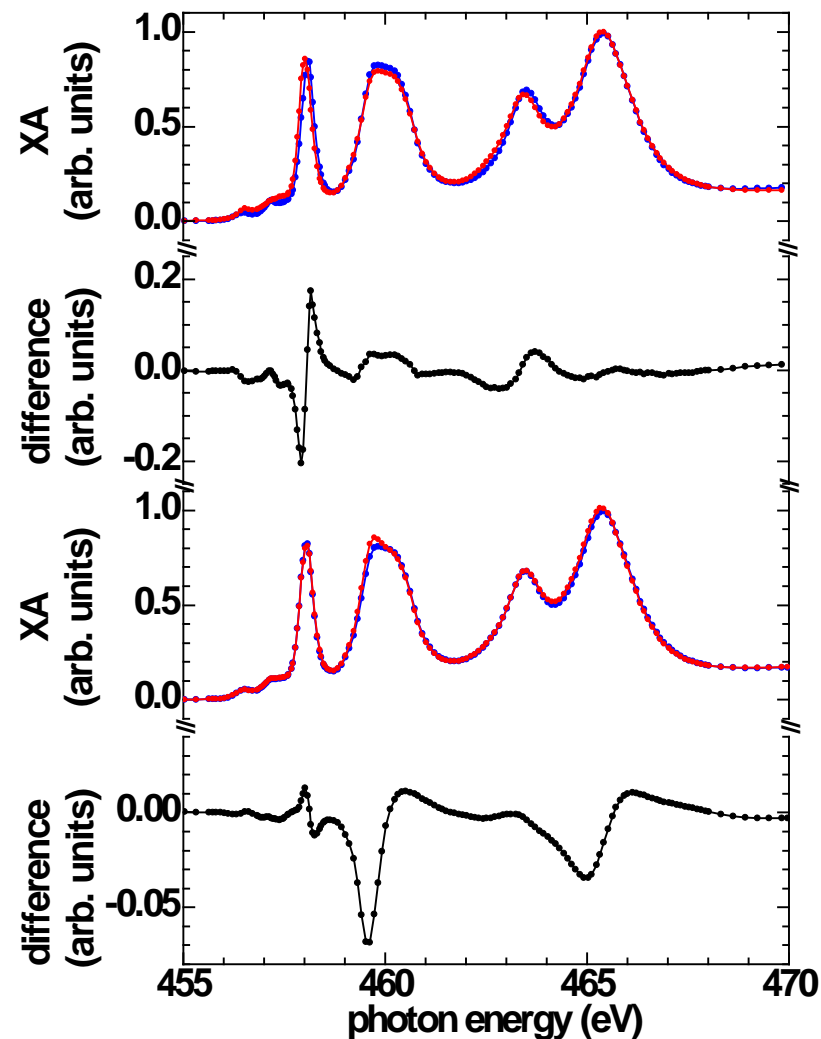


↑ ferroelectric polarization

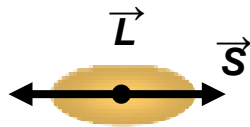


+ Spontaneous electric polarization due to off-center shift of $\text{Ti}^{4+}, \text{Zr}^{4+}$; associated with tetragonal distortion \Leftrightarrow linear dichroism

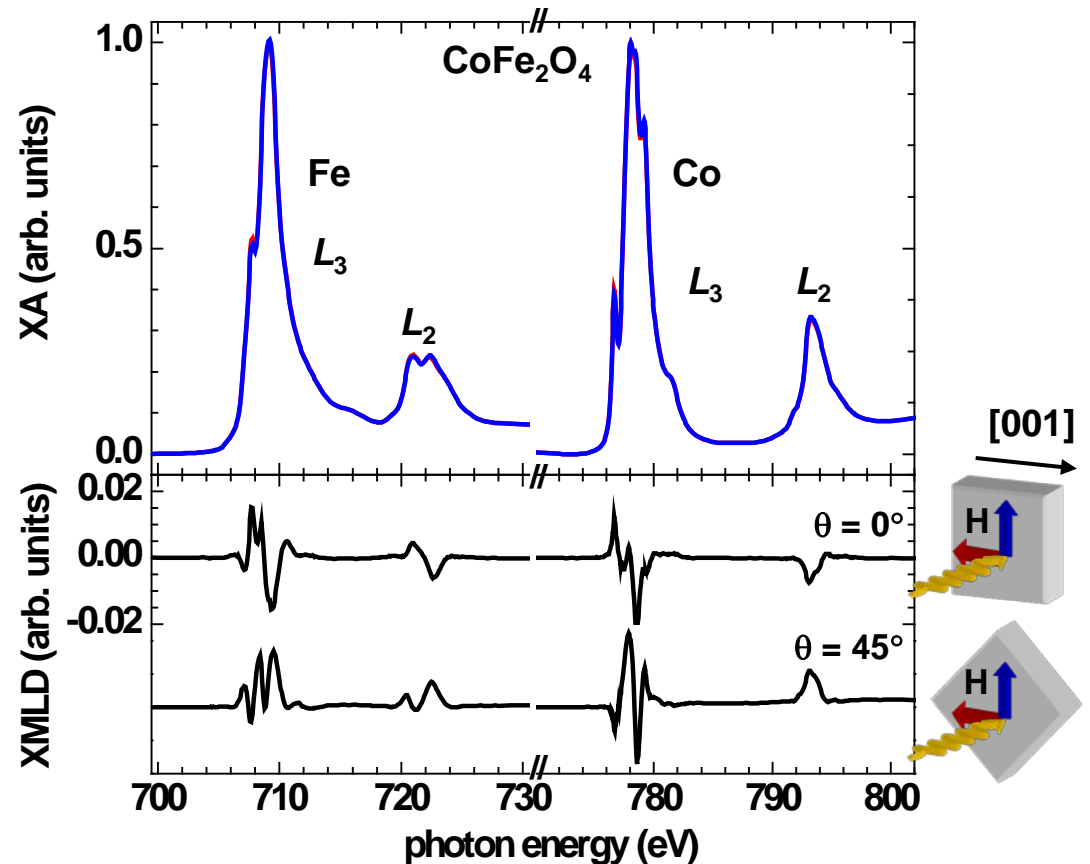
+ Reversing the polarization changes XA \Leftrightarrow Change in tetragonal distortion



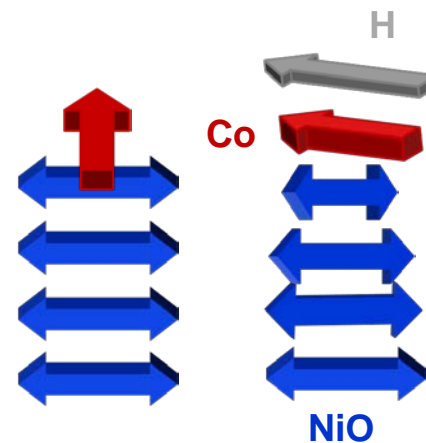
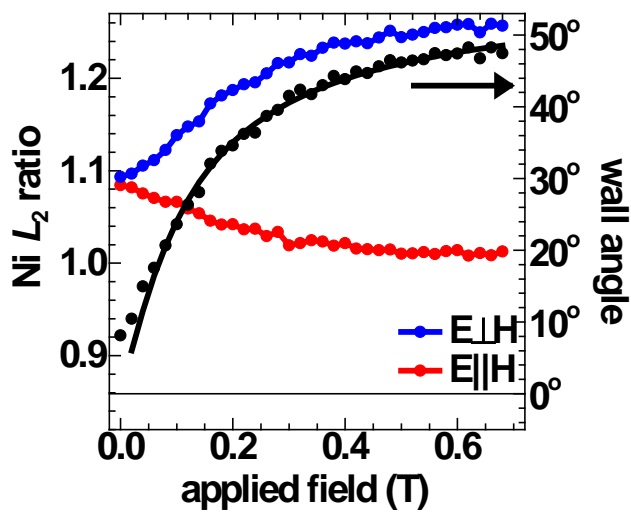
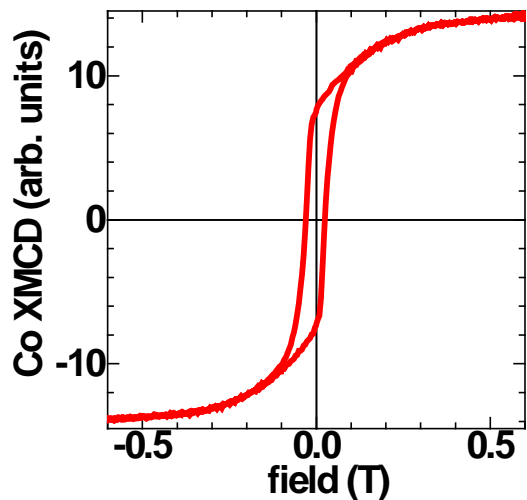
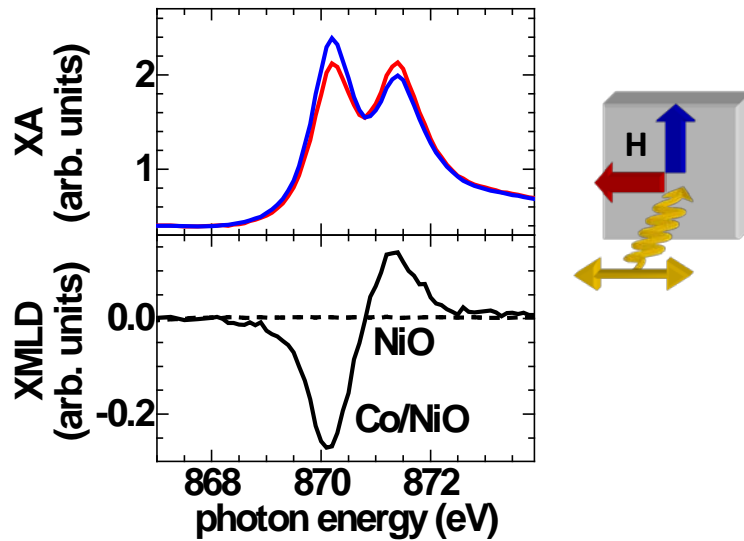
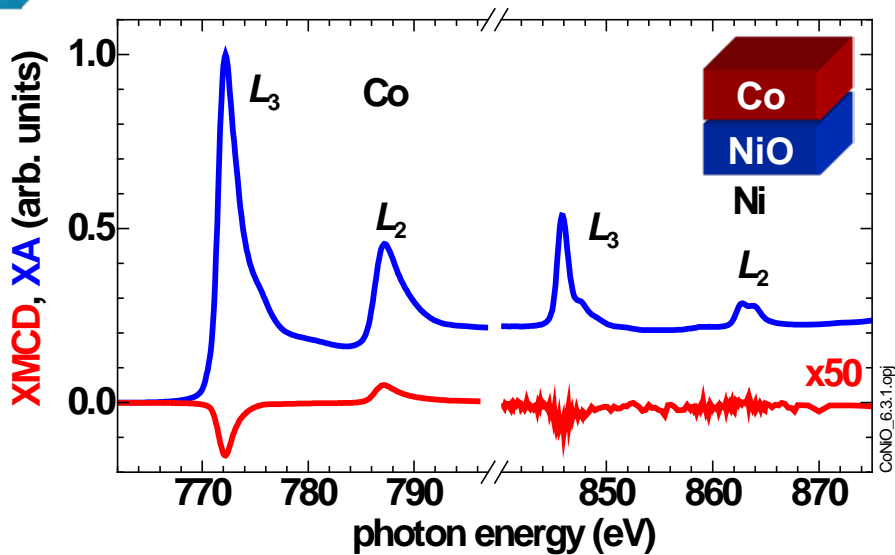
Isotropic d electron charge density
 \Rightarrow No polarization dependence



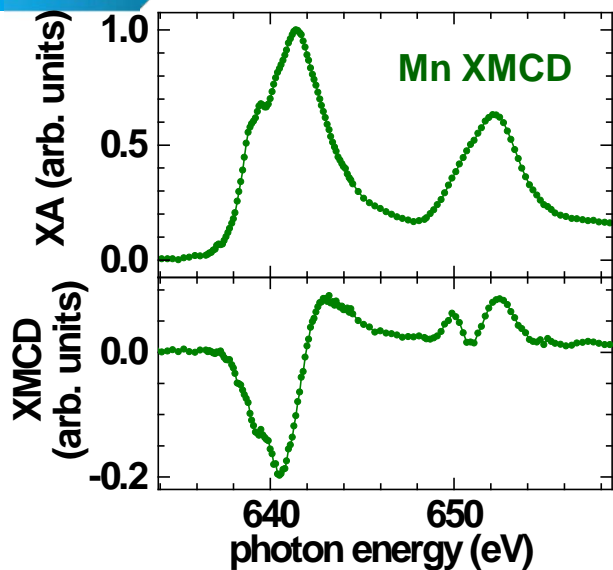
magnetically aligned
 Spin-orbit coupling distorts
 charge density
 \Rightarrow polarization dependence



- + $I_{\text{XMLD}} = I_{\parallel} - I_{\perp} \propto \langle m^2 \rangle$, $\langle m^2 \rangle =$ expectation value of the square of the atomic magnetic moment
- + XMLD allows investigating ferri- and ferromagnets as well as antiferromagnets.
- + XMLD spectral shape and angular dependence are determined by magnetic order and lattice symmetry.

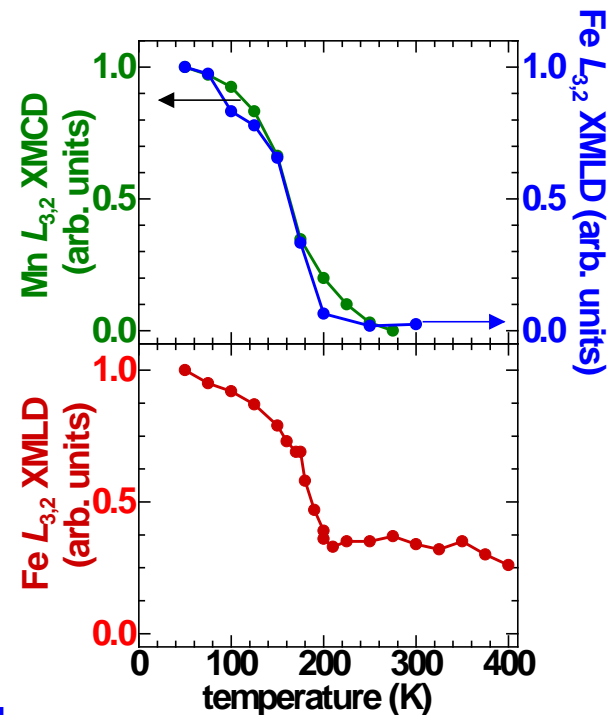
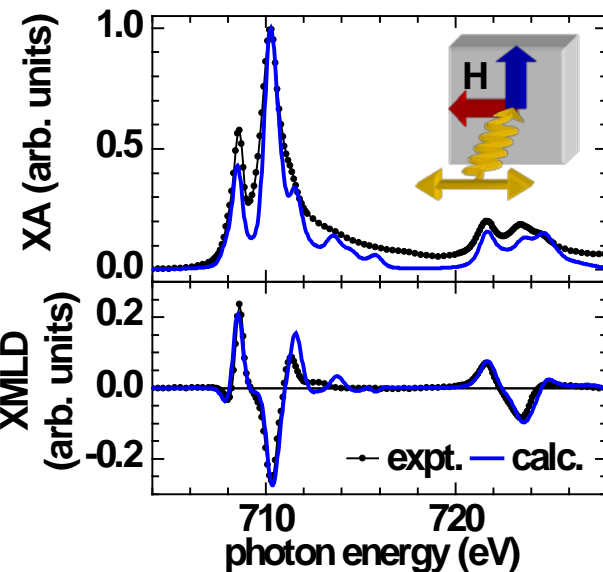
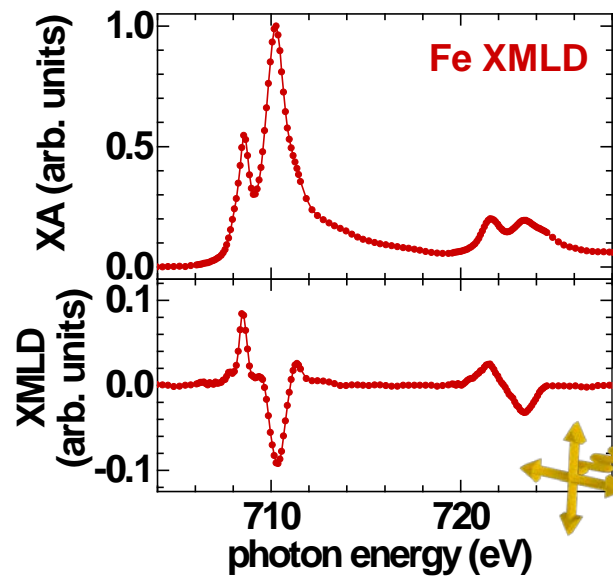


A. Scholl *et al.*,
Phys. Rev. Lett. 92, 247201 (2004)



$\text{La}_{0.7}\text{Sr}_{0.3}\text{MnO}_3$ (LSMO)
ferromagnet

$\text{La}_{0.7}\text{Sr}_{0.3}\text{FeO}_3$ (LSFO)
antiferromagnet

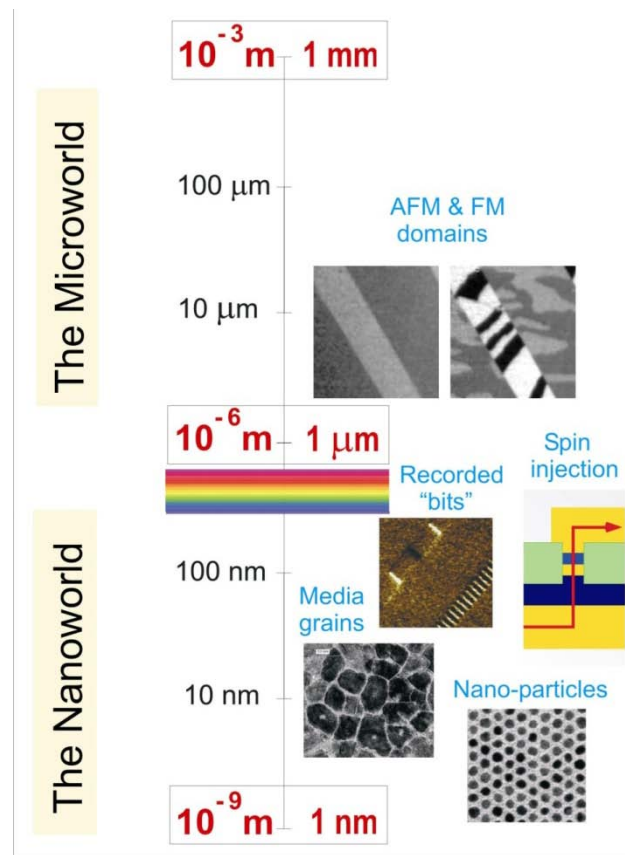
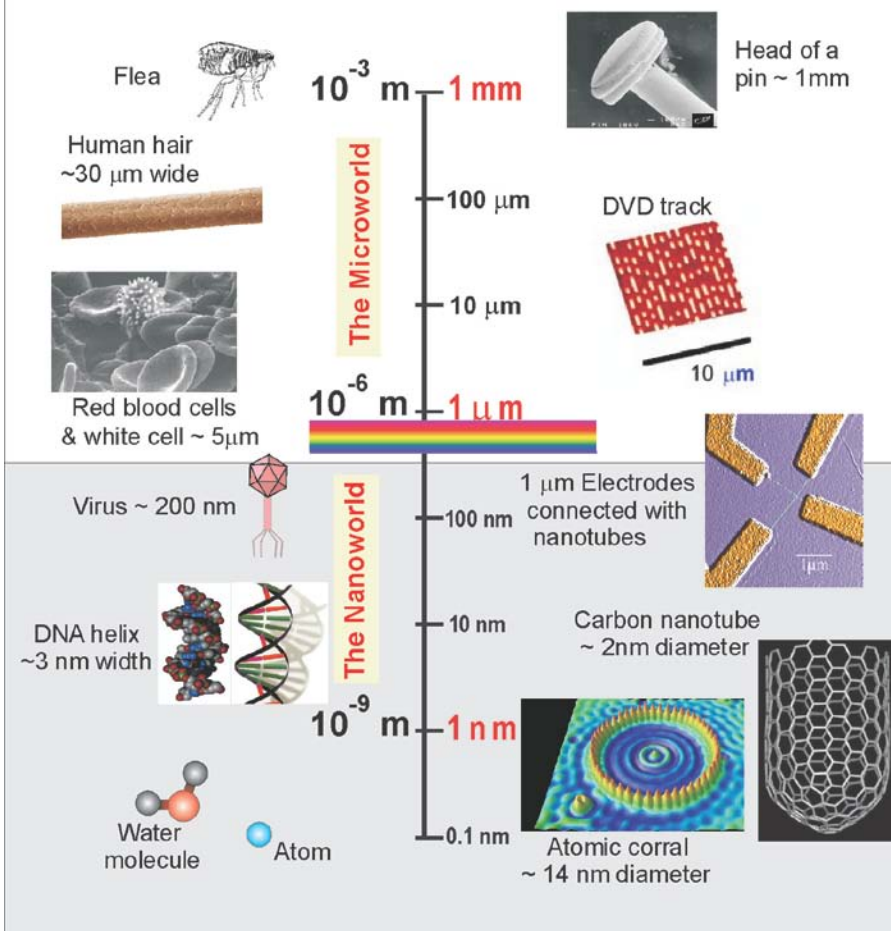


⇒ Perpendicular coupling
at LSMO/LSFO interface

Nature

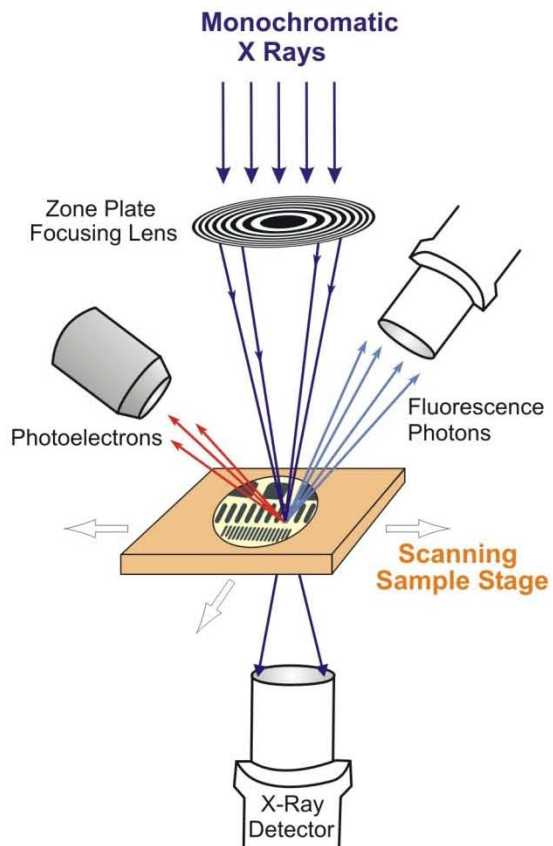
Technology

Magnetism

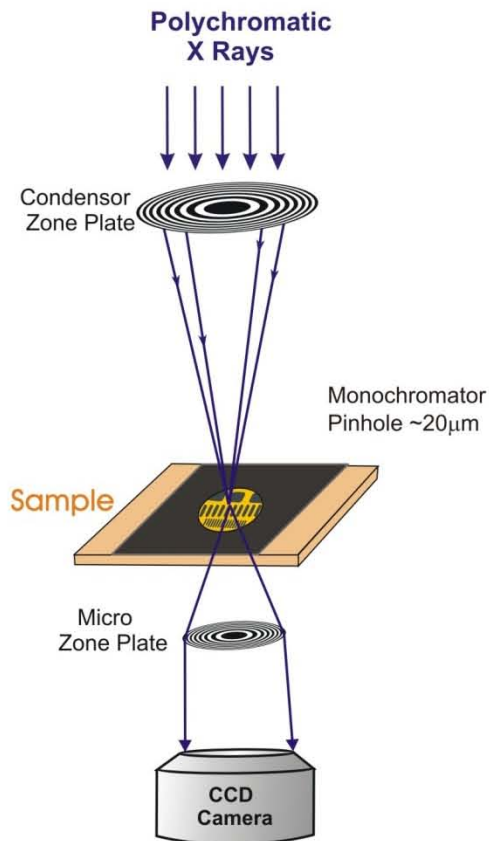


J. Stöhr, H.C. Siegmann,
Magnetism (Springer)

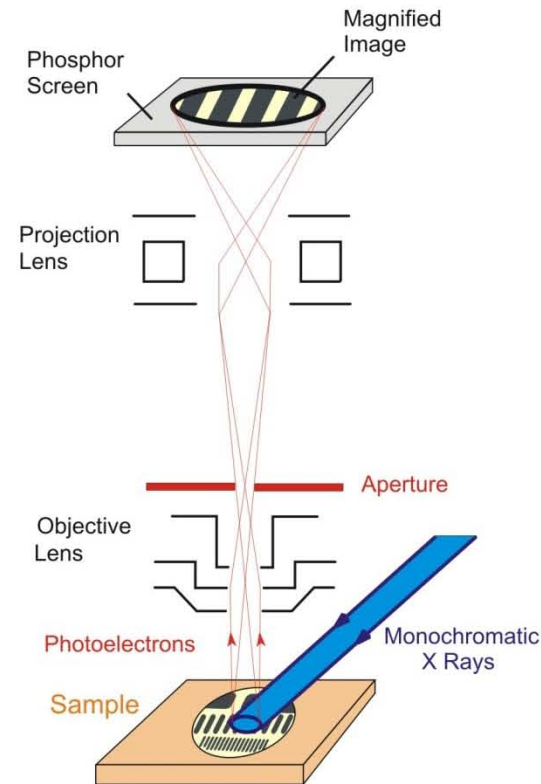
Scanning Transmission X-ray Microscopy STXM



Transmission X-ray Microscopy TXM

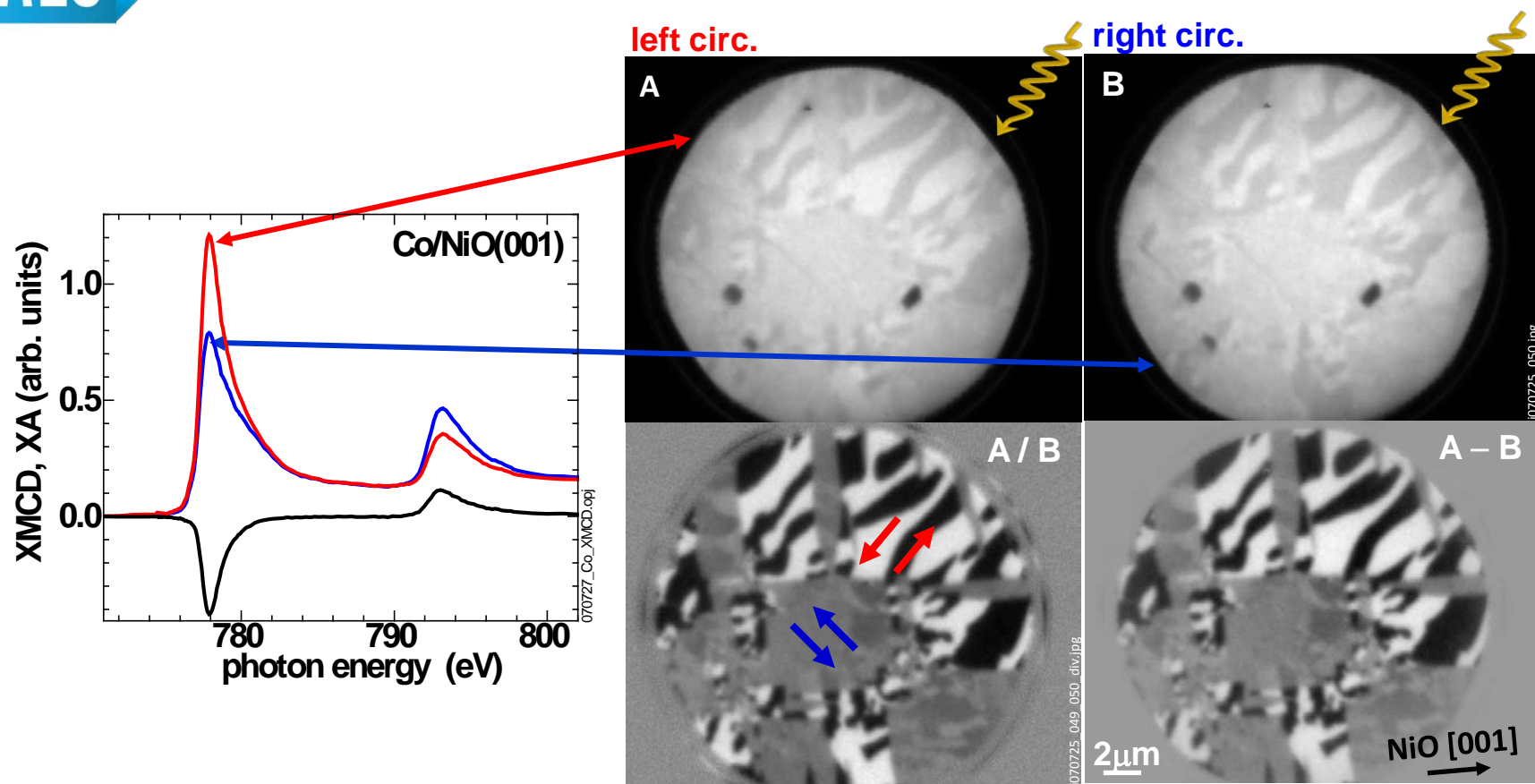


X-Ray Photoemission Electron Microscopy XPEEM

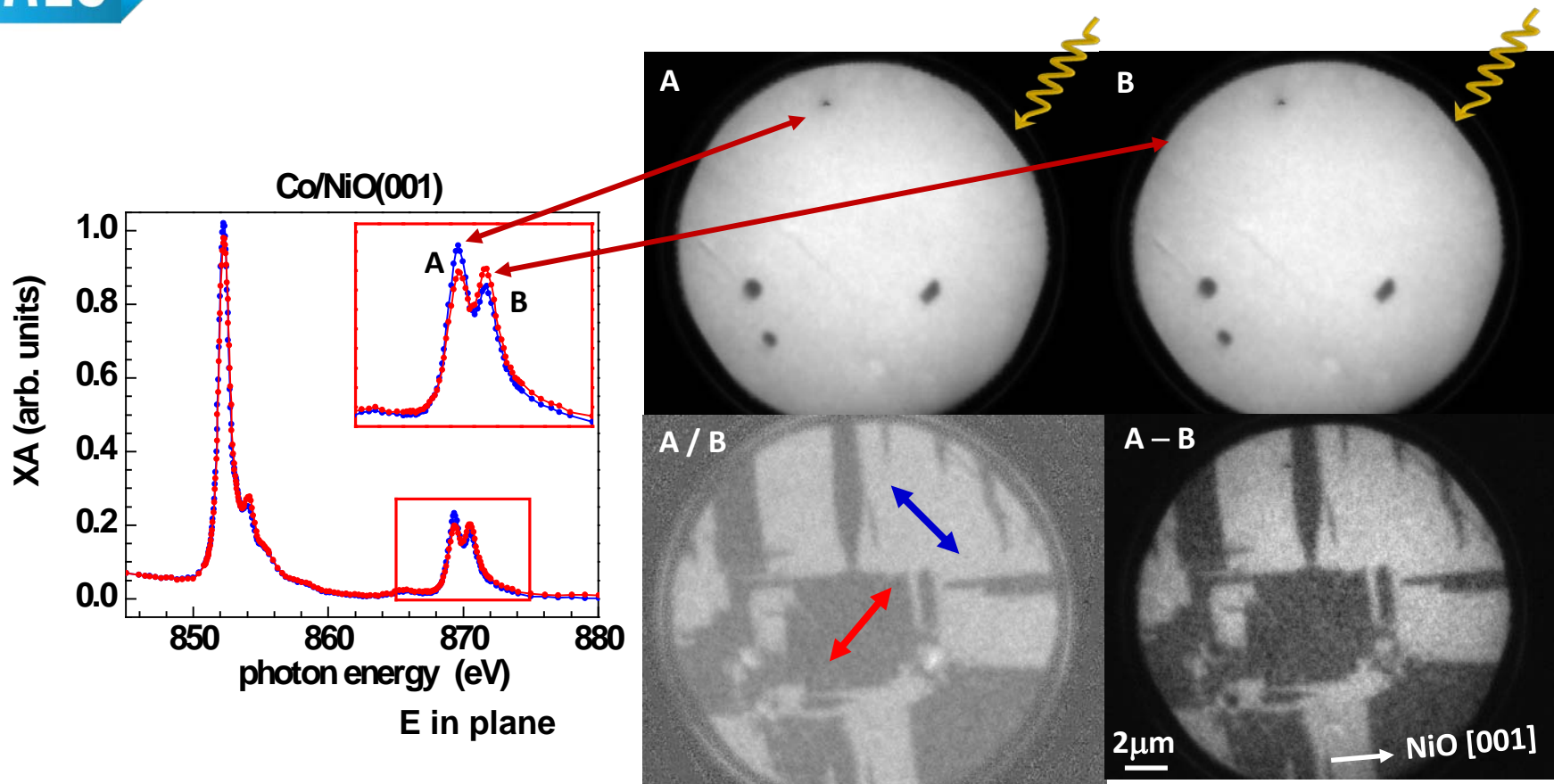


10-50 nm spatial resolution

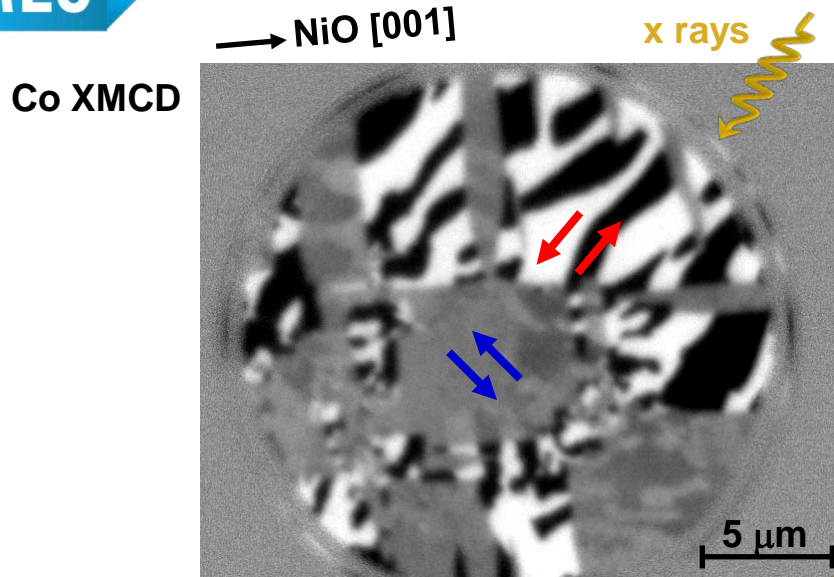
J. Stöhr, H.C. Siegmann,
Magnetism (Springer)



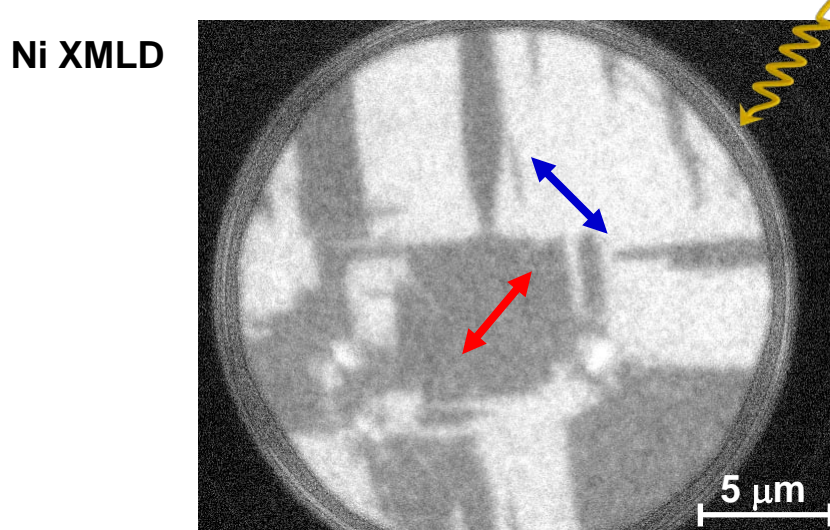
- + Images taken with left and right circularly polarized x-rays at photon energies with XMCD, i.e. Co L_3 edge, provide magnetic contrast and domain images.



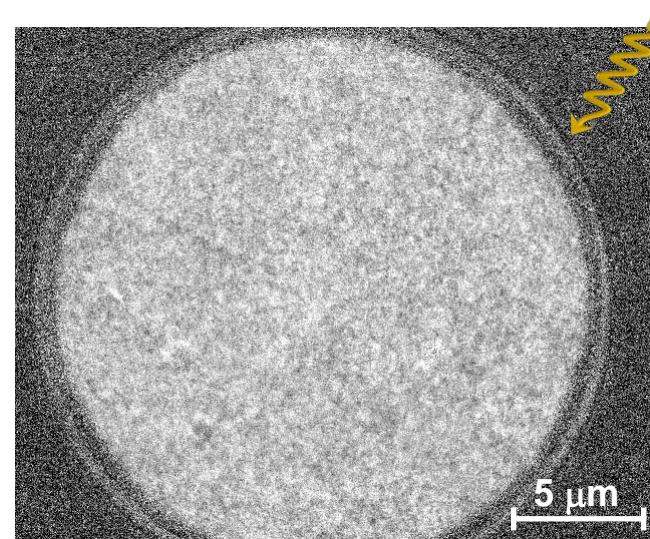
- + Images taken with linearly polarized x-rays at photon energies with XMLD, i.e. Ni L_2 edge, provide magnetic contrast and domain images.



- + Taking into account the geometry dependence of the Ni XMLD signal
⇒ perpendicular coupling of Co and NiO moments at the interface.



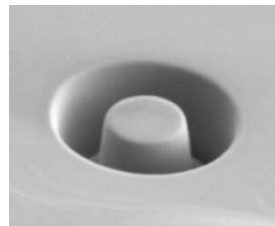
probing in-plane



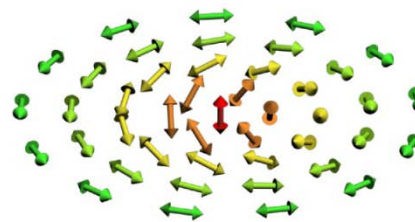
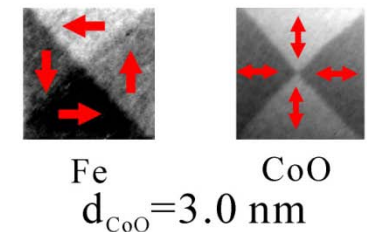
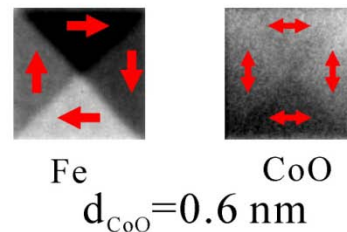
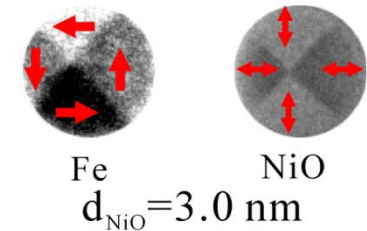
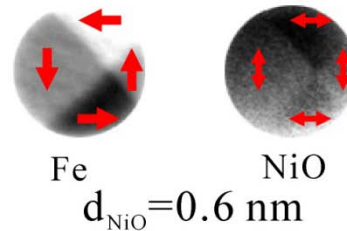
probing out-of-plane

+ First direct observation of vortex state in antiferromagnetic CoO and NiO disks in Fe/CoO and Fe/NiO bilayers using XMCD and XMLD.

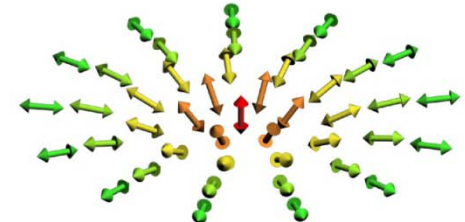
- + Two types of AFM vortices:
- conventional curling vortex as in ferromagnets
 - divergent vortex, forbidden in ferromagnets
 - thickness dependence of magnetic interface coupling



2 μm

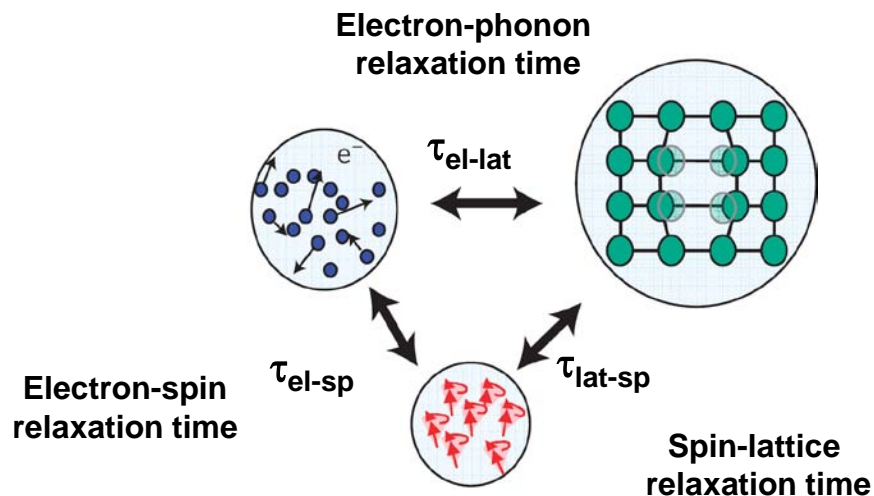
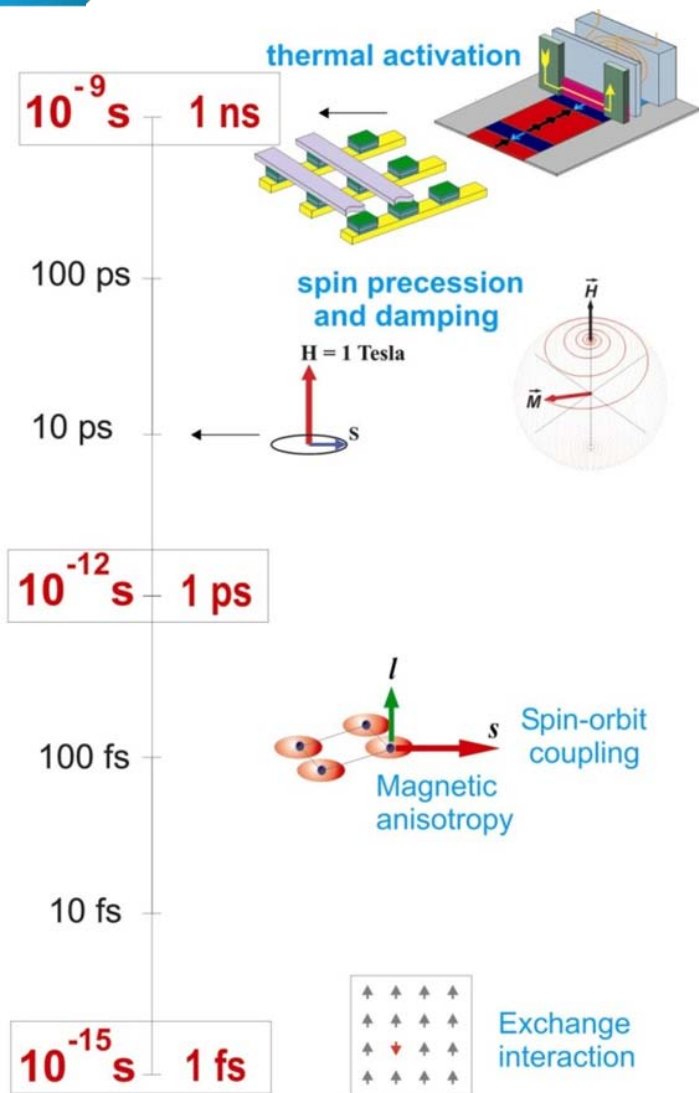


conventional curling vortex



divergent vortex

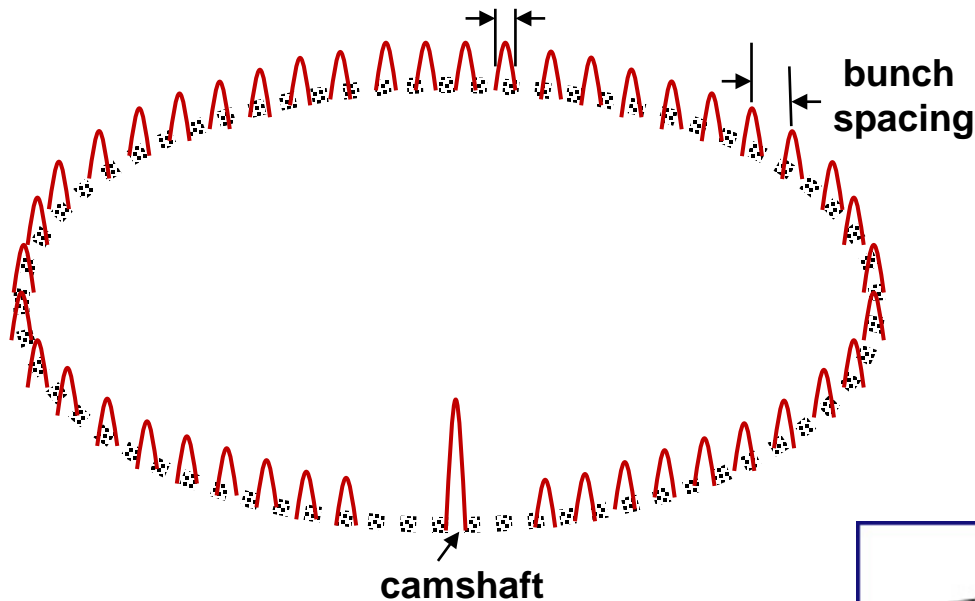
J. Wu *et al.*,
Nature Phys. **7**, 303 (2011)



- + Energy reservoirs in a ferromagnetic metal
- + Deposition of energy in one reservoir
- ⇒ Non-equilibrium distribution and subsequent relation through energy and angular momentum exchange

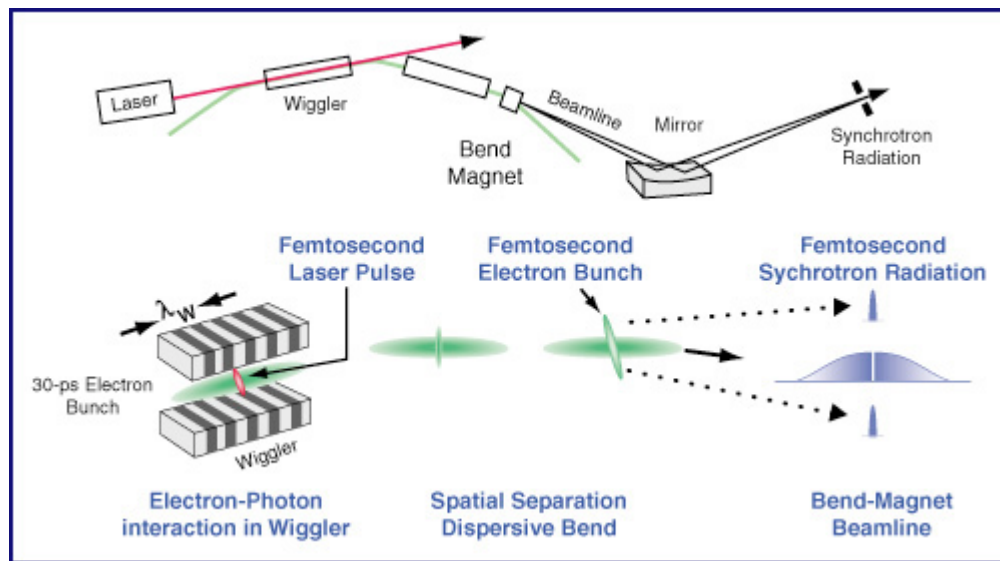
J. Stöhr, H.C. Siegmann,
Magnetism (Springer)

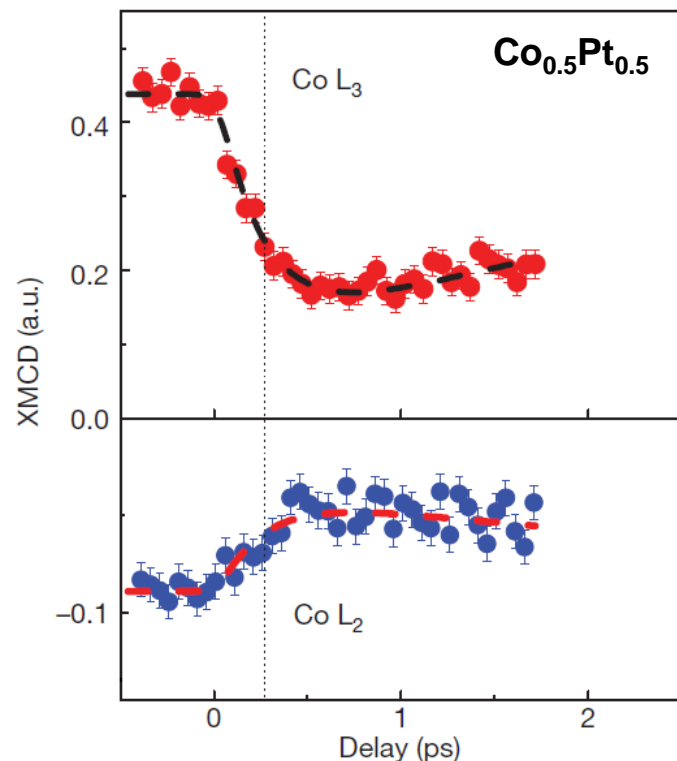
Pulse length 70 ps



- + 256-320 bunches for 500mA beam current
- + Possibility of one or two 5mA "camshaft" bunches in filling gaps
- + Bunch spacing:
multibunch mode: 2 ns
two-bunch mode: 328 ns
- + Pulse length 70ps

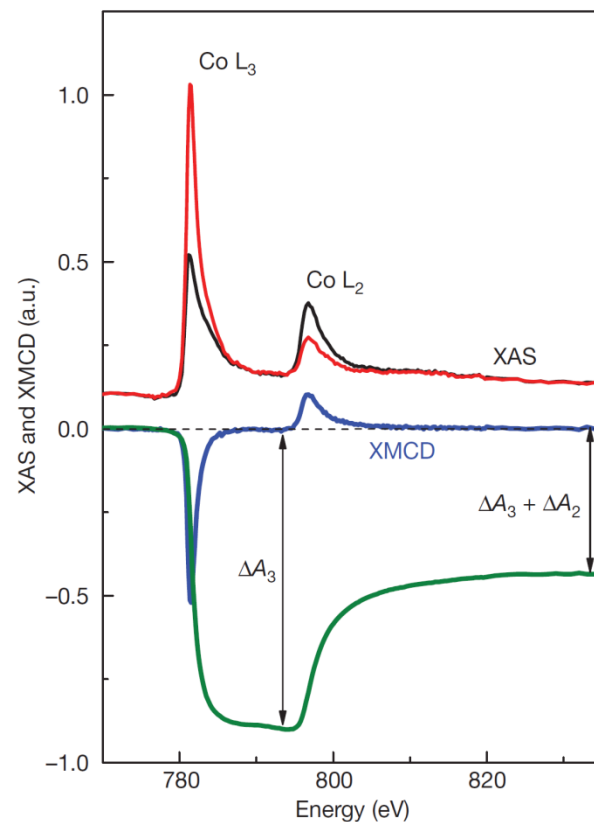
+ <300 fs x ray pulses though
"laser bunch-slicing technique"

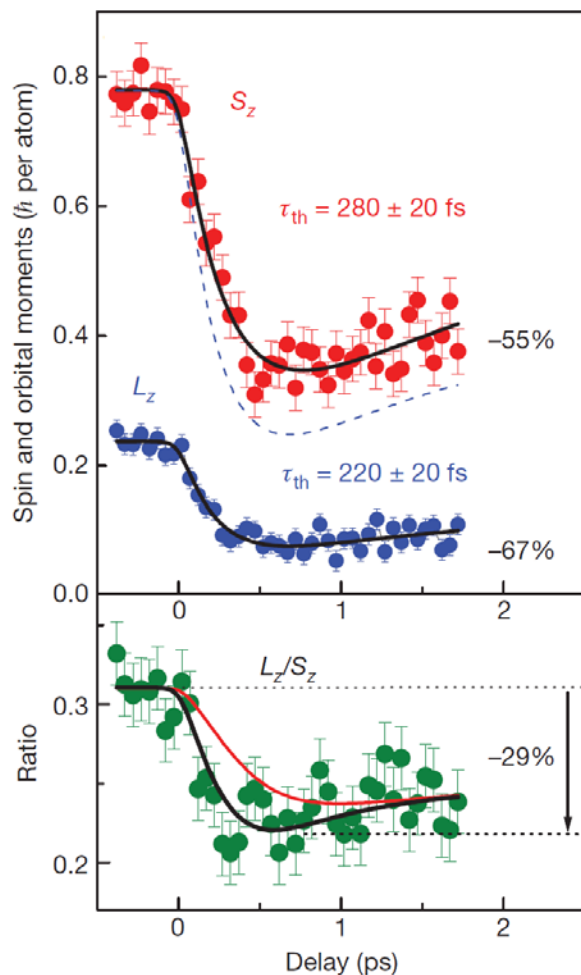




C. Boeglin, *et al.*,
Nature **465**, 458 (2010)

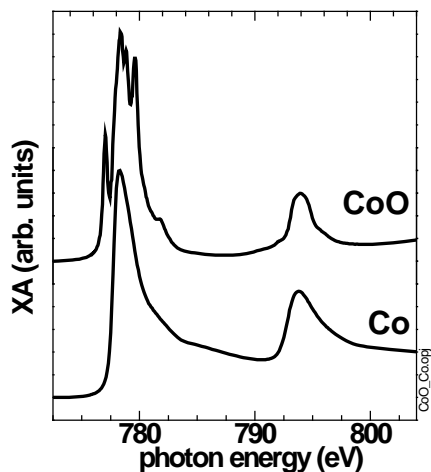
- + Orbital (L) and spin (S) magnetic moments can change with total angular momentum is conserved.
- + Efficient transfer between L and S through spin-orbit interaction in solids
- + Transfer between L and S occurs on fs timescales.
- + Co_{0.5}Pt_{0.5} with perpendicular magnetic anisotropy
- + 60 fs optical laser pulses change magnetization
- + Dynamics probed with XMCD using 120fs x-ray pulses
- + Linear relation connects Co L_3 and L_2 XMCD with L_z and S_z using sum rules



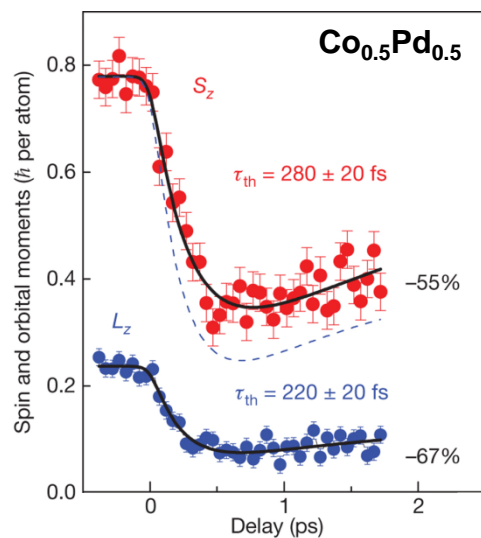
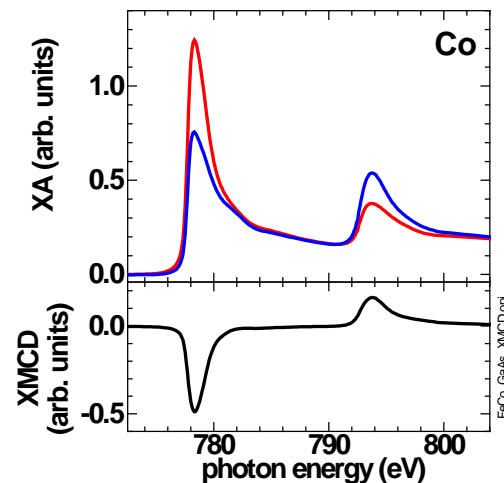


C. Boeglin, *et al.*,
 Nature 465, 458 (2010)

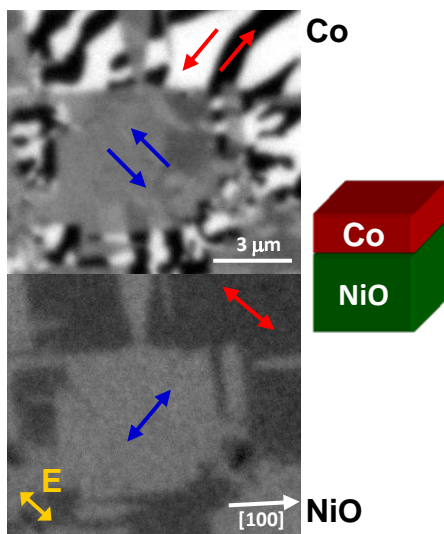
- + Characteristic thermalization:
 Faster decrease of orbital moment
- + Theory:
 Orbital magnetic moment strongly correlated with
 magnetocrystalline anisotropy
- + Reduction in orbital moment
 \Leftrightarrow Reduction in magnetocrystalline anisotropy
- + Typically observed at elevated temperatures in static
 measurements as well
- + Further studies needed



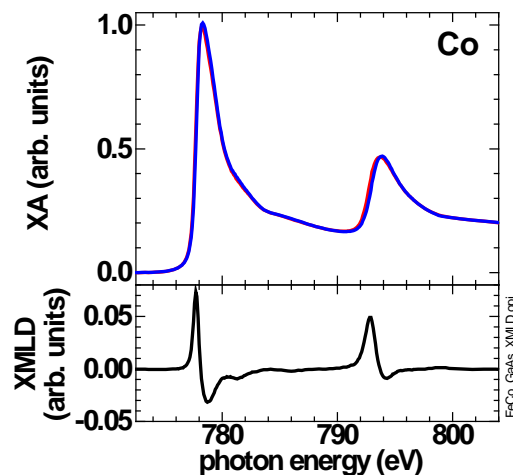
- + X ray absorption
- + X ray magnetic circular dichroism, XMCD
- + X ray magnetic linear dichroism, XMLD
- + X ray magnetic microscopy
- + Magnetization Dynamics

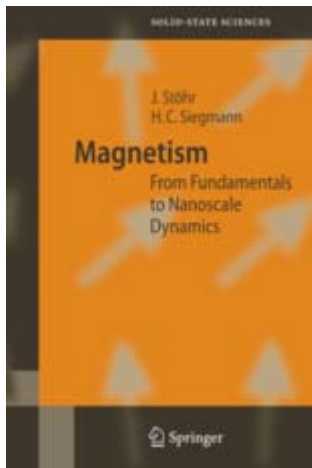


C. Boeglin *et al.*, Nature **465**, 458 (2011)

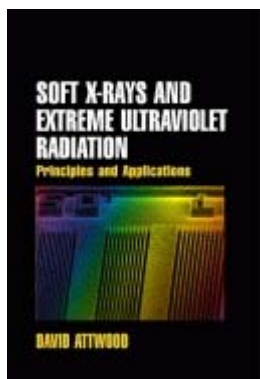


E. Arenholz *et al.*,
Appl. Phys. Lett. **93**, 162506 (2008)





J. Stöhr, H.C. Siegmann
Magnetism– From Fundamentals to Nanoscale Dynamics
Springer



D. Attwood
Soft X-Rays and Extreme Ultraviolet Radiation:
Principles and Applications